

Spring 5-2016

Stocks and Sources of Carbon Buried in the Salt Marshes and Seagrass Beds of Patos Lagoon, Southern Brazil

Elizabeth Weis Patterson
Bates College, epatter2@bates.edu

Follow this and additional works at: <http://scarab.bates.edu/honorsthesis>

Recommended Citation

Patterson, Elizabeth Weis, "Stocks and Sources of Carbon Buried in the Salt Marshes and Seagrass Beds of Patos Lagoon, Southern Brazil" (2016). *Honors Theses*. 170.
<http://scarab.bates.edu/honorsthesis/170>

This Open Access is brought to you for free and open access by the Capstone Projects at SCARAB. It has been accepted for inclusion in Honors Theses by an authorized administrator of SCARAB. For more information, please contact batesscarab@bates.edu.

Stocks and Sources of Carbon Buried in the Salt
Marshes and Seagrass Beds of Patos Lagoon
Estuary, Southern Brazil

An Honors Thesis

Presented to
The Faculty of the Department of Geology
Bates College

In partial fulfillment of the requirements for the
Degree of Bachelor of Science

by
Elizabeth Patterson

Lewiston, Maine
March 28, 2016

Abstract

This thesis investigates carbon source and stocks in salt marshes and seagrass beds in the Patos Lagoon estuary, the largest choked lagoon in the world, located in Southern Brazil. The study was conducted in the mesohaline region, at three shallow shoals. At each shoal, three sediment cores (50 cm deep) and plant biomass samples (aboveground and belowground) were collected along a transect line, spanning from the marsh to seagrass beds or unvegetated sediments (total = 9 sediment cores). The 50cm cores were subsampled and analyzed for organic carbon and nitrogen content, C/N ratios, and the isotope ratios of $^{13}\text{C}/^{12}\text{C}$, and $^{15}\text{N}/^{14}\text{N}$.

Geochemical data in marsh sediments generally reflect the overlying vegetation indicating that the carbon source is largely from the in situ vegetation. Seagrass and tidal flat sediments have similar isotopic signatures and likely represent a mix carbon source of seagrass, phytoplankton, and macroalgae. Sediments sampled closest to the city of Rio Grande (the largest populated area near the study site) are enriched in ^{15}N , which can be attributed to anthropogenic waste inputs into the lagoon.

Total carbon stocks for marshes (50cm depth) range from 97 to 221 MgC/ha. Seagrasses and tidal sediments have similar values and range from 9 to 57MgC/ha. These estimates are comparable to global values and indicate the importance of these ecosystems as carbon sinks. Initial rough calculations of ecosystem carbon stocks for the total area of marshes and seagrass beds in Patos Lagoon are 2,900,000 to 6,600,000 MgC and 210,000 to 680,000 MgC, respectively. The size of these stocks emphasize the fact that these ecosystems are significant uncouncted carbon sinks in Brazil that should be conserved and potentially utilized in Brazil's active carbon market.

Acknowledgments

This project would not have been possible without the support of a number of people.

I would like to acknowledge the generous funding from the Bates Student Research Fund and the Bates College Geology Department.

I would also like to thank the Bates College Geology Department. My experiences with the department have forever changed academics from a chore into a passion.

The biggest possible thank you to my advisor, Bev Johnson, who has been a person of endless support and guidance throughout this whole process. I have had the privilege to see the enthusiasm she has for her students and science since my freshman year at Bates. She has introduced me to field that I have grown to love and has equipped me with the skills to go out and pursue it. Another huge thank you to Margareth Copertino. This project would not have been possible without her support and generous welcome into her lab at the Institute of Oceanography at the Federal University of Rio Grande.

To Phil Dostie: Thank you for all of your support in lab and your unbelievable patience with all of the complications along the way. I would also like to thank Carini, Vanessa, and Milikku for their help out in the field and in back in lab. Thank you Edu and Rafa, who were the best hosts I ever could have asked for during for my time in Brazil.

Thank you to my fellow seniors, with whom I have spent endless ours in the library and Coram. Let's set a goal to spend a little more time outside.

A final shout out to my family. In particular, Mom, thank you for your continued support through all of my ups and downs this year. You have always been a role model and have truly inspired me to pursue science throughout college and beyond.

Table of Contents

Introduction	1
1.1 Importance of Salt Marshes and Seagrasses	2
1.2 Threats	3
1.3 Carbon in Salt Marshes and Seagrasses	3
1.3.1 Coastal Carbon Cycle	3
1.3.2 Carbon Storage in Salt Marshes and Seagrass Beds	3
1.3.3 Blue Carbon in Marshes and Seagrass Beds	3
1.4 Stable Isotope Geochemistry	4
1.4.1 Stable isotopes	4
1.4.2 Delta notation	4
1.4.3 Fractionation	5
1.4.4 C/N ratio	7
1.5 Using lead concentrations to determine sedimentation rates	7
1.6 Carbon Source and Storage in Brazil	8
1.7 Purpose	8
1.8 Study Site	8
1.8.1 Physical characteristics of the Patos-Mirim lagoon system	8
1.8.2 Geologic Setting	9
1.8.3 People and Patos Lagoon	9
Methods	10
2.1 Overview	11
2.2 Field Work in Patos Lagoon	11
2.2.1 Sediments	11
2.2.2 Plants	14
2.3 Sample Preparation	14
2.3.1 Sediments	14
2.3.2 Plants	14
2.4 Inductively Coupled Plasma Atomic Optical Emission Spectrometry (ICP-OES)	14
2.5 Elemental Analyzer-Isotope Ratio Mass Spectrometer (EA-IRMS)	15
2.6 Bulk Density and Carbon Density	15
2.7 Carbon Stocks	15
2.7.1 Carbon in Aboveground and Belowground Biomass	15
2.7.2 Sediment	16
2.7.3 Total Carbon Stock	16
Results	17
3.1 Plant Geochemistry	18
3.2 Core descriptions	19
3.2.1 Transect 1	19
3.2.2 Transect 2	19
3.2.3 Transect 3	20
3.3 Downcore Trends	20
3.3.1 Transect 1	20

3.3.2 Transect 2	30
3.3.3 Transect 3	31
3.4 Carbon Density	31
3.5 Sedimentary Lead Concentrations.	31
Discussion	33
4.1 Plant Biplot	34
4.2 Carbon Source	35
4.2.1 Transect 1	35
4.2.2 Transect 2	36
4.2.3 Transect 3	36
4.3 Enriched $\delta^{15}\text{N}$	38
4.4 Carbon Sequestration	40
4.4.1 The History of Leaded Gasoline as an Age Model	40
4.4.2 Carbon Burial Rates.	40
4.5 Carbon Stocks	42
4.5.1 Biomass	42
4.5.2 Sediments.	44
4.5.3 Total Carbon Stock	45
4.6 Significance	46
References	48
Appendices.	53
Appendix 1	54
Appendix 2	58
Appendix 3	67

Table of Figures

Figure 1.1: A map showing the global distribution of seagrasses, salt marshes, and mangroves (from Pendleton et al., 2012). 2

Figure 1.2: A schematic of carbon sources in a marsh and seagrass bed ecosystem. Arrows denote movement of carbon. 5

Figure 1.3: A cross-section of a salt marsh highlighting the typical zones, vegetation, and isotopic signature (from Johnson et al., 2007). 6

Figure 1.4: A location map of Patos Lagoon with an inset map of the Patos Lagoon Estuary (from Odebrecht et al., 2010). The dark line denotes the channel through the estuary. 9

Figure 2.1: A) Coring device with 7.5cm diameter tube and removable top B) A sediment core in the casing with the top removed, packed with cloth and styrofoam, and caps placed on top and bottom . 12

Figure 2.2: Site map of Patos Lagoon with Transects 1, 2, 3, outlined in red boxes. Inset maps show detailed image of each transect with each core location shown with a blue dot. Images taken from Google Earth, 2015. 13

Figure 3.1: A biplot of the $\delta^{15}\text{N}$ (‰) vs $\delta^{13}\text{C}$ (‰) for all sampled plants (*Spartina densiflora*, *Juncus* spp, *Scirpus maritimus*, *Ruppia maritima*). Values plotted are averages with standard deviation. 20

Figure 3.2: Stratigraphic log of T1-1 in leftmost panel. Geochemical data plotted against depth(cm) from left to right are %C, Bulk Density (g/cm^3), C/N ratios, $\delta^{13}\text{C}$ (‰), and $\delta^{15}\text{N}$ (‰). 23

Figure 3.3: Stratigraphic log of T1-3 in leftmost panel. Geochemical data plotted against depth(cm) from left to right are %C, Bulk Density (g/cm^3), C/N ratios, $\delta^{13}\text{C}$ (‰), and $\delta^{15}\text{N}$ (‰). 24

Figure 3.4: Stratigraphic log of T1-5 in leftmost panel. Geochemical data plotted against depth(cm) from left to right are %C, Bulk Density (g/cm^3), C/N ratios, $\delta^{13}\text{C}$ (‰), and $\delta^{15}\text{N}$ (‰). 25

Figure 3.5: Stratigraphic log of T2-1 in leftmost panel. Geochemical data plotted against depth(cm) from left to right are %C, Bulk Density (g/cm^3), C/N ratios, $\delta^{13}\text{C}$ (‰), and $\delta^{15}\text{N}$ (‰). 26

Figure 3.6: Stratigraphic log of T2-3 in leftmost panel. Geochemical data plotted against depth(cm) from left to right are %C, Bulk Density (g/cm^3), C/N ratios, $\delta^{13}\text{C}$ (‰), and $\delta^{15}\text{N}$ (‰). 27

Figure 3.7: Stratigraphic log of T2-5 in leftmost panel. Geochemical data plotted against depth(cm) from left to right are %C, Bulk Density (g/cm^3), C/N ratios, $\delta^{13}\text{C}$ (‰), and $\delta^{15}\text{N}$ (‰). 28

Figure 3.8: Stratigraphic log of T3-1 in leftmost panel. Geochemical data plotted against depth(cm) from left to right are %C, Bulk Density (g/cm^3), C/N ratios, $\delta^{13}\text{C}$ (‰), and $\delta^{15}\text{N}$ (‰). 29

Figure 3.9: Stratigraphic log of T3-3 in leftmost panel. Geochemical data plotted against depth(cm) from left to right are %C, Bulk Density (g/cm^3), C/N ratios, $\delta^{13}\text{C}$ (‰), and $\delta^{15}\text{N}$ (‰). 30

Figure 3.10: Stratigraphic log of T3-5 in leftmost panel. Geochemical data plotted against depth(cm) from left to right are %C, Bulk Density (g/cm^3), C/N ratios, $\delta^{13}\text{C}$ (‰), and $\delta^{15}\text{N}$ (‰). 31

Figure 3.11: A graph of average carbon density (gC/cm^3) for each core to a depth of 50cm with standard deviation. Blue bars are cores from Transect 1, orange bars are cores from Transect 2, and green bars are cores from Transect 3. 34

Figure 3.12: Sediment lead concentrations(ppm) plotted vs depth(cm) for core T1-3. 34

Figure 4.1: A biplot of $\delta^{13}\text{C}$ (‰) and $\delta^{15}\text{N}$ (‰) of measured isotopic values of plant samples with literature values of C3 and C4 plants (O’Leary, 1998; Peterson and Fry, 1987), phytoplankton (Goericke and Fry, 1994; Peterson and Fry, 1987), seagrasses (Kennedy et al., 2010 and Papadimitriou et al., 2005), macroalgae (Harris et al., 2016 (Unpublished)), and benthic microalgae (Weinstein et al., 2000).....36

Figure 4.2: A biplot of $\delta^{13}\text{C}$ (‰) and $\delta^{15}\text{N}$ (‰) showing sediment samples from Transect 1 plotted as dots. Average isotopic values of vegetation samples are plotted with standard deviation as ovals.39

Figure 4.3: A biplot of $\delta^{13}\text{C}$ (‰) and $\delta^{15}\text{N}$ (‰) showing sediment samples from Transect 2 plotted as dots. Average isotopic values of vegetation samples are plotted with standard deviation as ovals.39

Figure 4.4: A biplot of $\delta^{13}\text{C}$ (‰) and $\delta^{15}\text{N}$ (‰) showing sediment samples from Transect 3 plotted as dots. Average isotopic values of vegetation samples are plotted with standard deviation as ovals.40

Figure 4.5: A map of the main sources of aquatic contamination in the Patos Lagoon Estuary (taken from Almeida et al., 1993; Tagliani et al., 2003). Inset map denotes area around Transect 1.41

Figure 4.6: Carbon burial rates ($\text{gC}/\text{m}^2/\text{yr}$) from offshore cores of Transects 1-3. Literature values of burial rates of different ecosystems taken from Mcleod et al., 2011. Note log scale.....43

Figure 4.7: Average aboveground and belowground biomass (MgC/ha) for each species plotted with standard deviation.....45

Figure 4.8: Total carbon stocks for each site are given by combining living biomass (aboveground) and sediment carbon (sediment and belowground) values (MgC/ha). Literature values for unvegetated (Choi and Wang, 2004), marsh (Elsley-Quirk et al., 2011; Howard et al., 2014), Seagrass (Howard et al., 2014), boreal forest, temperate forest, and tropical forest (Fourqurean et al., 2012).....47

Table of Tables

Table 1.1: Literature values of $\delta^{13}\text{C}$ and $\delta^{15}\text{N}$ of primary producers	7
Table 2.1 Species collected for biomass at each core site * not analyzed in this study*	14
Table 3.1: Average $\delta^{13}\text{C}$ (‰), $\delta^{15}\text{N}$ (‰), C/N ratios, and standard deviation for all plant species	21
Table 3.2: Average carbon density (gC/cm^3) to 50cm depth with standard deviation for each sediment core.	34
Table 4.1 Carbon burial rates for offshore sediment cores	43
Table 4.2 Carbon content for all plant species (MgC/ha)	45
Table 4.3 Carbon stocks (MgC/ha) of sediments, biomass, and total in upper 50cm of sediment	46
Table 4.4 Total ecosystem carbon stock (MgC/ha) for marshes and seagrass beds in upper 50cm of sediment.	48

Introduction

1.1 Importance of Salt Marshes and Seagrasses

Tidal salt marshes and seagrass beds are two ecosystems that are found along the coast around the world (Figure 1.1). In general sea grasses are more globally distributed whereas salt marshes are confined to more temperate latitudes (Orth et al., 2006). Simply defined, a salt marsh is an area of coastal grassland that is regularly flooded by seawater. A seagrass bed is defined as a bed of marine grasses found just below low-tide line. The total global area of salt marshes is 22,000-400,000km² whereas the global area of seagrasses is slightly larger at 117,000-600,000km² (McLeod et al., 2011). While these two ecosystems occupy less than 1% of coastal ocean area, they provide greater ecosystem services than many marine and terrestrial environments (Farber et al., 1997). These ecosystems provide habitat to many different organisms and are nurseries for some commercial fisheries. Seagrasses in particular are an important food source and habitat for megaherbivores and commercially important fish (Beck et al., 2001). The extensive root systems of these coastal ecosystems stabilize soils making them energy buffers that protect coastlines from strong waves and storm events.

These ecosystems sequester and store carbon at very high levels with average global carbon burial rates of 218 (+/- 24)gCm⁻²yr⁻¹ and 138 (+/-38)gCm⁻²yr⁻¹ for salt marshes and seagrasses, respectively (McLeod et al., 2011). Salt marshes and seagrass beds also efficiently store carbon at 278 and 111 MgC/ha, respectively (Elsey –Quirk et al., 2011; Howard et al., 2014).

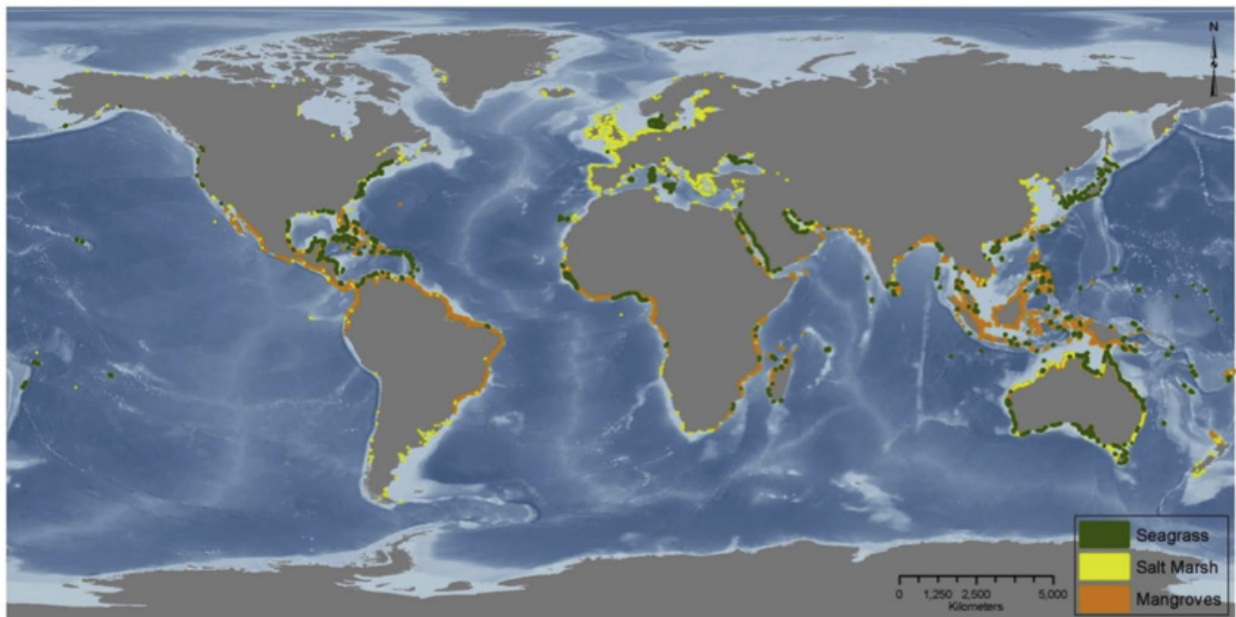


Figure 1.1: A map showing the global distribution of seagrasses, salt marshes, and mangroves (from Pendleton et al., 2012).

1.2 Threats

Increasing human population and economic development has put increased pressure on coastal resources, which negatively affects many fragile coastal ecosystems. Both marshes and seagrasses exist on the margin between land and sea making them susceptible to small environmental changes from multiple different sources. Marsh loss has largely been due to drainage and coastal development. Seagrass reduction and dieback has been particularly prominent in recent years due to acute causes such as eutrophication, dredging, and fishing as well as global changes in precipitation, temperature, and freshwater discharge (Orth et al., 2006). To date 35% of the historical tidal marsh range and 29% of the seagrass range has been lost (Howard et al., 2014). An additional 30-40% of unprotected salt marshes and seagrass beds could be lost in the next 100 years if human behavior is not modified (Pendleton et al., 2012).

1.3 Carbon in Salt Marshes and Seagrasses

1.3.1 Coastal Carbon Cycle

It has been found that terrigenous inputs of organic matter into marine sediments have been underestimated in the Gulf of Mexico and elsewhere (Prahl and Muehlhausen, 1989; Goni et al., 1997). This underestimate is particularly true for sediments deposited at the coastal margins. The depositional nature of coastal margins results in preferential burial conditions for terrigenous organic matter relative to marine organic matter (Hedges et al., 1988; Hedges, 1992). This is largely due to terrigenous sediments spending less time in the water column and undergoing rapid burial rates (Muller and Suess, 1979; Emerson and Hedges 1988). Carbon cycling and carbon source is still not well constrained in many coastal areas and further research is needed to understand the dynamics of these ecosystems.

1.3.2 Carbon Storage in Salt Marshes and Seagrass Beds

The nature of salt marsh and seagrass ecosystems make them good carbon sinks. High carbon drawdown rates and subsequent storage of biomass in the roots and rhizomes result in high rates of vertical accretion of organic rich sediments (Chmura et al., 2003). Anoxic soil conditions in both of these ecosystems prevent much of the deposited organic matter from being decomposed. This, combined with the vertical accretion of sediments, causes the carbon sink to grow with time. It has been shown that carbon can accumulate in these ecosystems for thousands of years, creating long-term carbon sinks (Iacono et al., 2008).

1.3.3 Blue Carbon in Marshes and Seagrass Beds

In recent years increasing greenhouse gas concentrations in the atmosphere and increasing global temperatures have been linked to anthropogenic climate change. There has been a subsequent push to evaluate how to best combat these changes and reduce the damages that could result. Carbon sequestration has been recognized as a powerful tool for removing CO₂ from the atmosphere. A carbon sink can be beneficial to the environment because it stores atmospheric CO₂ in a form that does not affect the radiative balance of the Earth. However, when damaged or destroyed, a carbon sink can easily become a carbon source (McLeod et al., 2011). There has been a recent push to look for strategies that

take advantage and preserve ecosystems that sequester greenhouse gases (Canadell and Raupach, 2008). This has led to increased attention for ecosystems that are known carbon sinks.

Salt marshes, seagrass beds, and mangroves have recently been called coastal blue carbon ecosystems (United Nations Environment, 2010). This term was invented in an effort to bring new attention to ecosystems that were previously unrecognized for their carbon sequestration storage potential. Generally defined, blue carbon is the carbon found in mangroves, tidal salt marshes, and seagrass beds, which includes the aboveground, belowground, as well as the non-living biomass (McLeod et al., 2011).

In both marshes and seagrass beds, there are often multiple different inputs of carbon to the system other than the carbon deposited in situ (Figure 1.2). This is largely due to the fact that these ecosystems have complex root systems and canopies making them good at trapping sediments (Howard et al., 2014). Seagrasses efficiently remove particles from the water column due to collisions with the plant structure (Hendriks et al., 2008). Marsh shoots similarly trap particles at high tide and their rhizomes create sediment stability, which further facilitates the incorporation of foreign organic matter (Leonard and Luther, 1995; Middelburg et al., 1997). Salt marshes and seagrass beds also host a variety of primary and secondary producers, which all add to the supply of organic matter deposited locally (Vizzini et al., 2002). All of these carbon sources can be lumped into two primary groups, autochthonous carbon (carbon produced in situ) and allochthonous carbon (carbon incorporated from outside sources).

These two groups of carbon create an interesting complication when counting blue carbon. Autochthonous would represent the carbon deposited from the marsh plants and seagrasses themselves. However, allochthonous carbon is also a big factor in coastal ecosystems due to the fact they are located in hydrodynamically active settings (waves, tides, rivers, and currents) which allow for the transport and introduction of foreign carbon (Howard et al., 2014). This creates a problem when the total carbon sequestered by the ecosystem is counted. If allochthonous carbon is counted both at its source and at its site of deposition, then the carbon is being counted twice. This could lead to overestimates of the carbon sinks within the global carbon cycle, which emphasizes the importance of the determination of carbon source in these ecosystems.

One approach to this issue is to look at the geochemical properties of the carbon sediments buried in salt marshes and seagrass beds. To help differentiate carbon source sources, techniques such as C/N ratios and stable isotopes ratios, such as $^{13}\text{C}/^{12}\text{C}$ and $^{15}\text{N}/^{14}\text{N}$, can be used (Peterson and Fry, 1987; Fry et al., 1977; Middelburg et al., 1997; Johnson et al., 2007; Kennedy et al., 2010).

1.4 Stable Isotope Geochemistry

1.4.1 Stable isotopes

Isotopes are variations of the same element with different numbers of neutrons resulting in differing mass numbers. Isotopes that do not undergo radioactive decay are called stable isotopes. There are two naturally occurring stable isotopes of carbon, ^{12}C and ^{13}C , which have an abundance of 98.89% and 1.11%, respectively. Similarly, nitrogen also has two stable isotopes, ^{14}N and ^{15}N , which have an abundance of 99.636% and 0.364%, respectively.

1.4.2 Delta notation

Delta notation, given as ‰, is used to present stable isotope composition. It is the ratio of the heavy to the light isotope in a sample relative to a standard multiplied by 1,000, as follows:

$$\delta X = \left[\left(\frac{R_{\text{sample}}}{R_{\text{standard}}} \right) - 1 \right] * 1000$$

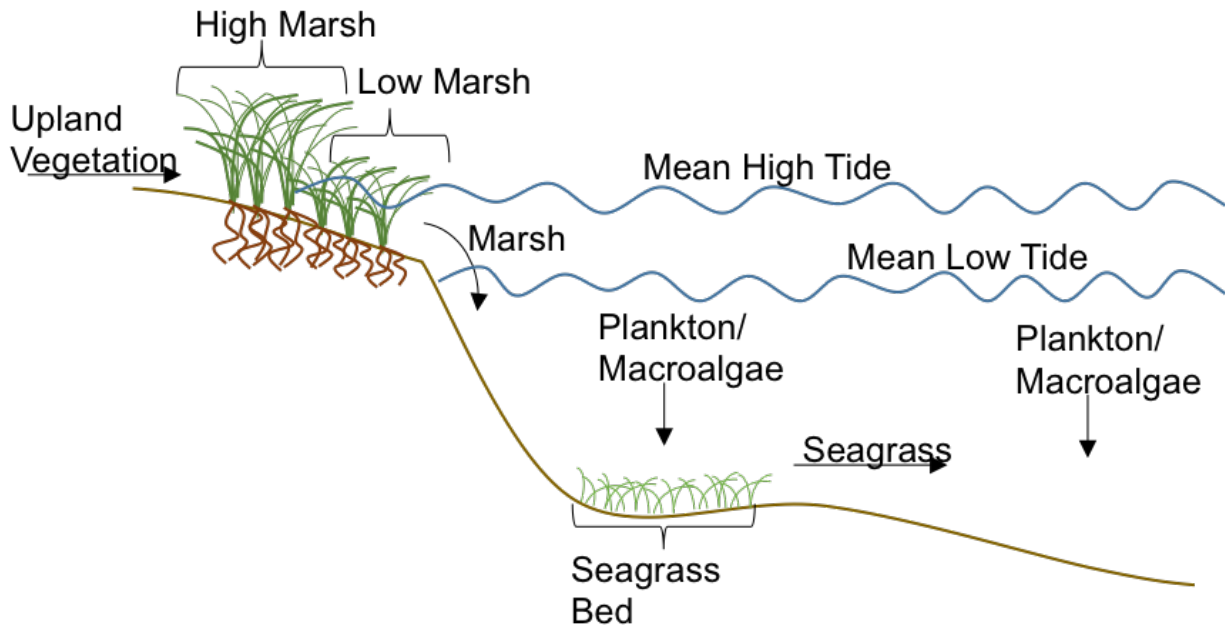


Figure 1.2: A schematic of carbon sources in a marsh and seagrass bed ecosystem. Arrows denote movement of carbon.

Where X signifies ^{13}C or ^{15}N and R corresponds to $^{13}\text{C}/^{12}\text{C}$ and $^{15}\text{N}/^{14}\text{N}$, ratios. The standards used for carbon and nitrogen are Pee Dee Belemnite (or Vienna PDB) and nitrogen gas in the atmosphere, respectively. High values signify that the sample is enriched with heavy isotopes, whereas a low value is enriched in the light isotope.

1.4.3 Fractionation

Isotope fractionation is the process by which the relative abundance of isotopes in a substance is affected. Kinetic fractionation is a type of fractionation where isotopes are separated by their mass due to a unidirectional process. Biochemical reactions often result in kinetic fractionation because the pathways are largely unidirectional pathways, resulting in a preferential selection against heavier isotopes (Galimov, 2012). In photosynthesis, for example, when CO_2 is taken up by plants, $^{12}\text{CO}_2$ is preferred over $^{13}\text{CO}_2$ because it takes less energy to break $^{12}\text{CO}_2$ bonds and form simple sugars than to break $^{13}\text{CO}_2$ bonds. Plants are thus relatively depleted in heavier isotopes compared to inorganic materials (Tyson, 1995). Some plants are more selective than others causing some to have a lower $^{13}\text{C}/^{12}\text{C}$ ratio. Plants that employ C_3 photosynthesis select for the lighter isotope and have lower $\delta^{13}\text{C}$ values (-27‰) whereas plants that employ C_4 photosynthesis are not as selective and have higher $\delta^{13}\text{C}$ values (-14‰) (Table 1.1).

Salt marshes in New England have been characterized by elevation and hydroperiod into low marsh (regularly inundated) and high marsh (irregularly inundated) zones (Nixon, 1982). There is a general shift from C_4 to increasing C_3 plants across a transect from low to high marsh (Figure 1.3). The lower marsh is dominated by C_4 plants, such as *Spartina* spp, due to their increased tolerance to anoxic and saline soils. C_3 plants, such as *Juncus* spp populate the high and higher high marsh and *Scirpus* spp, largely populating the brackish to fresh waters of the higher marsh (Johnson et al., 2007). This vegetation gradient causes the isotopic signature of carbon from high and low marsh zones to be very different (Chmura and Aharon, 1995; Choi et al., 2001).

The nitrogen cycle is more complex than the carbon cycle resulting in more factors that affect

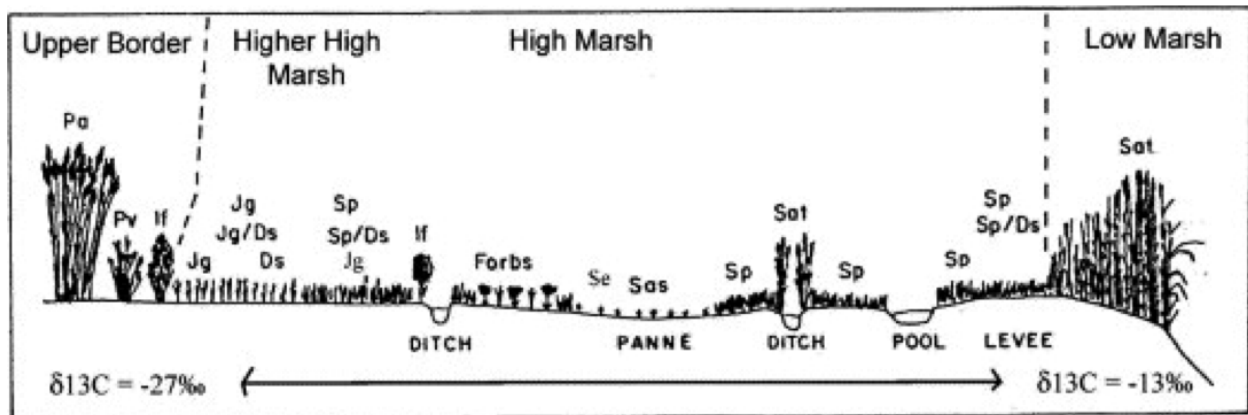


Figure 1.3: A cross-section of a salt marsh highlighting the typical zones, vegetation, and isotopic signature (from Johnson et al., 2007).

the $\delta^{15}\text{N}$ signal of organic matter. Plants assimilate nitrogen through their roots and rhizomes in the form of nitrate. Fractionation due to assimilation in primary producers, ranging from -27 to 0‰, can be highly variable and is controlled by the initial concentrations of nitrate, diffusion rates through cell walls, and enzymes (Sharp, 2007). In general, plants preferentially select for the lighter isotope, ^{14}N , over the heavy isotope, ^{15}N , during assimilation. Marsh plants and seagrasses follow this trend and have $\delta^{15}\text{N}$ values that are generally enriched in ^{15}N , with a range of -3 to 8‰ (Peterson and Fry, 1987; Papadimitriou et al., 2005; Kennedy et al., 2010). The $\delta^{15}\text{N}$ signal of sediments depends on the original $\delta^{15}\text{N}$ values of the plants and modification due to microbial decomposition, and generally ranges from 3 to 12‰ (Schoeninger and DeNiro, 1984; Tiessen et al., 1984; Fogel and Cifuentes, 1993). Fractionation due to microbial decomposition is roughly 1 to 2‰.

The $\delta^{15}\text{N}$ signal of a plant can be altered by a variety of factors. Aerobic bacteria select against ^{15}N during denitrification (a process by which nitrate is ultimately converted to N_2 gas) resulting in nitrate enriched in ^{15}N relative to baseline levels. High rates of primary production can also cause plants to be less selective with nitrate and result in an enriched signal (Fogel and Cifuentes, 1993).

Anthropogenic inputs such as human and animal waste or fertilizer have significantly different signals from naturally occurring soil and plant nitrogen and can alter the signal of nitrogen in groundwater and surface waters (Fogel and Cifuentes, 1993; Macko, 1994). Organic fertilizer from animal waste and sewage are enriched in ^{15}N relative to natural plant and soil values and have values ranging from 10 to 20‰ (Kreitler and Browning, 1983). Furthermore, inputs of untreated waste have been shown to increase the $\delta^{15}\text{N}$ values of plants in salt marshes and estuarine ecosystems (Cole et al., 2004; Cole et al., 2005). In contrast, inorganic fertilizers have been shown to decrease $\delta^{15}\text{N}$ values in soils and plants because they are derived from atmospheric nitrogen, which has a $\delta^{15}\text{N}$ value of 0‰ (Macko, 1994).

All of these different environmental factors can alter the nitrogen signal measured in plant matter or sediments. This makes determining organic matter source complicated when solely using $\delta^{15}\text{N}$. However, it has been shown that nitrogen isotopes can be useful when applied in combination with carbon values for tracing the source of carbon in sediments (Peterson et al., 1985).

There are several primary producers that dominate the salt marsh and seagrass bed ecosystems. The typical stable carbon and nitrogen isotope values for the main primary producers are given in Table 1.1. These values are of use because the isotopic composition of sediments can be used to try to constrain the source of organic matter.

1.4.4 C/N ratio

Plant type	$\delta^{13}\text{C}$	$\delta^{15}\text{N}$	Citation $\delta^{13}\text{C}$	Citation $\delta^{15}\text{N}$
C3 (high marsh)	-28‰	-3 to +8‰	(Peterson and Fry, 1987)	(Peterson and Fry, 1987)
C4 (low marsh)	-14‰	-2 to +2‰	(Johnson et al., 2007; Peterson and Fry, 1987)	(Peterson and Fry, 1987)
Plankton	-22‰	-2 to 11‰	(Goericke and Fry, 1994)	(Peterson and Fry, 1987)
Seagrass	-18‰	+2 to +6‰	(Kennedy et al., 2010; Papadimitriou et al., 2005)	(Kennedy et al., 2010; Papadimitriou et al., 2005)
Macroalgae	-17‰	+5 to +8‰	(Harris et al., 2016 (unpublished))	(Harris et al., 2016 (unpublished))
Benthic Microalgae	-17‰	+5 to 11‰	Weinstein et al., 2000	Weinstein et al., 2000

In addition to isotopic ratios, elemental analysis of organic matter has also been successfully utilized to distinguish between vascular and planktonically derived organic matter preserved in sediments (Meyers, 1997). It is another factor to help determine the source of organic carbon in a sediment sample by looking at previously known values. C/N ratios derived from phytoplankton usually fall between 4 and 10, whereas terrestrial land plants have normal values above 20 (Meyers, 1994). This difference is largely due to the absence of cellulose in algae and the high amount in vascular plants (Meyers, 1997). For the purposes of this study, these categories (vascular vs. planktonic) have been more broadly defined as macroplants (C/N>10), such as higher plants and macroalgae, and microplants (C/N<10), such as phytoplankton and benthic microalgae.

1.5 Using lead concentrations to determine sedimentation rates

An understanding of the sedimentation rate allows for the carbon burial rate to be calculated and the sedimentation history of a core to be determined. Several different methods have been used for calculating sedimentation rates. Radiometric data using ^{210}Pb or ^{137}Cs has been used to date coastal sediments (Chanton et al., 1983; Niencheski et al., 2014), however, these methods are often expensive.

An alternative way to calculate sedimentation rate is to measure the concentration of heavy metals in sediment and match the vertical variations to known anthropogenic historical inputs, such as leaded gasoline emissions (Cendy et al., 1997; Sarkar et al., 2015). This technique has been successfully employed in the United States where most of the lead found in recent sediments originates from the deposition of lead gasoline byproducts. Leaded gasoline became relatively standard use worldwide in the 1920s (Davies and Alloway, 1990). Use of leaded gasoline in the United States increased until its phaseout with the initiation of the Clean Air Act in 1970 (Juracek and Ziegler, 2006). This resulted in a 99.8% decrease of the use of leaded gasoline from 1970-1990 (USEPA, 2000). These relatively abrupt changes in lead concentrations are reflected in the sediments, where lead settles out of the water column,

allowing a sedimentation rate to be determined for the recent past.

It has been shown that salt marshes and tidal flats, with minimal mixing, are both environments where heavy metal concentrations can be matched to anthropogenic pollution history (Cundy and Croudace, 1996; Lee and Cundy, 2001). This suggests that these ecosystems are an area where stable lead concentrations could potentially be used as a cheaper means for calculating sedimentation rates.

1.6 Carbon Source and Storage in Brazil

Brazil has one of the world's longest coastlines at over 7,000km (Odebrecht et al., 2010). With nearly 20,000 hectares of seagrass beds and extensive marshes, the coasts of Brazil have a large carbon sink that has been largely understudied (Da Silva Copertino, 2011). Brazil has long been a leader of protecting carbon sinks by valuing its largest terrestrial sink, the Amazon rainforest, being the first nation to sign the United Nations Framework on Climate Change, and supporting the Kyoto Protocol (Trennepohl, 2010). Programs like Reducing Emissions from Deforestation and Forest Degradation (REDD) have been successful in preserving large portions of forest by giving them commercial value and bringing Brazil to the forefront of the global carbon market. However, salt marshes and seagrass beds remain the least studied carbon source in the country, but hold the potential to be both environmentally and commercially important carbon sinks in Brazil. With increased knowledge of the scope and carbon storage capacity of these coastal ecosystems, Brazil could see large economic benefits and would be forced to reconsider conservation policies for these ecosystems. One potential carbon sink is in Patos Lagoon in southern Brazil. This lagoon is home to both salt marshes and seagrass beds and learning more about their carbon source and storage could help inform about the carbon cycle and sink capacity of the lagoon system.

1.7 Purpose

One of the goals of this project is to characterize the source of the organic carbon in transects of sediment cores taken from salt marshes to shallow waters in Patos Lagoon in Rio Grande, Brazil. Stable isotopes and C/N ratios will be used to determine the source(s) of organic matter in 50cm sediment cores from three different environments across each transect, salt marsh, seagrass bed, and deeper sediments. A sedimentation rate from one core will be determined using lead concentrations. Bulk density, %C, and the sedimentation rate will be used to estimate the rate at which carbon is sequestered at these sites.

1.8 Study Site

1.8.1 Physical characteristics of the Patos-Mirim lagoon system

The Patos-Mirim lagoon system is located in Rio Grande do Sul, Brazil's southernmost state and drains a 200,000km² watershed (Seeliger and Kjerfve, 2000) (Figure 1.4). It is the world's largest choked coastal lagoon with a length of 250km, an average width of 40km, and total surface area of 10,360km² (Kjerfve, 1986; Fernandes et al., 2002). It is a river-dominated lagoon with tidal influence restricted to the area near the ocean (Moller et al., 1996). This is largely due to its restricted outlet to the Atlantic Ocean which is a 0.8km wide channel and 15m deep inlet that is constrained by 4km jetties built and designed in the early twentieth century to stabilize the inlet for the city of Rio Grande (Odebrecht et al., 2010). The water level of the lagoon is highly variable and can change for long periods of time. Salinity also fluctuates regularly and can range from 0 to 35ppm (Niencheski et al., 2014). In times of flood or El Niño

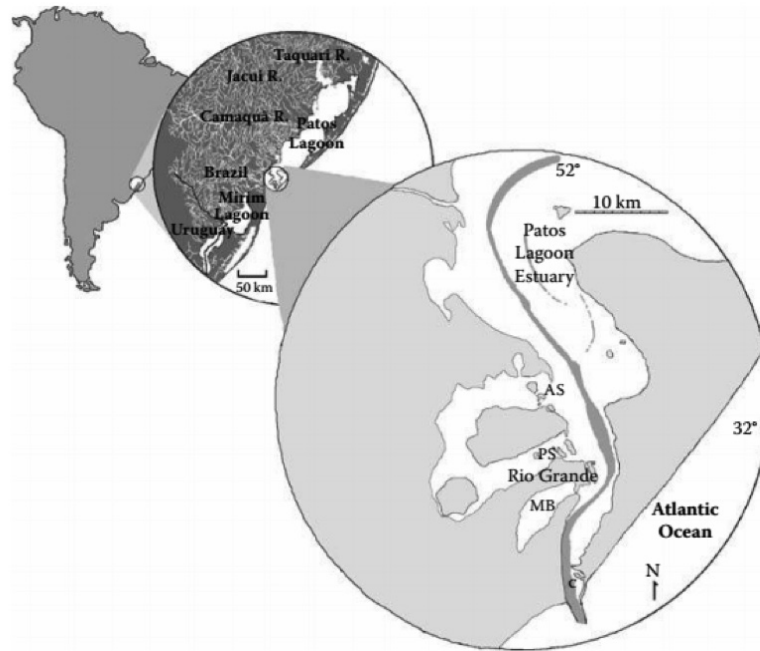


Figure 1.4: A location map of Patos Lagoon with an inset map of the Patos Lagoon Estuary (from Odebrecht et al., 2010). The dark line denotes the channel through the estuary.

years, increased precipitation and water levels can freshen the lagoon for months at a time (Grimm et al., 1998; Moller et al., 2001). In the summer months, seawater penetration into the lagoon is increased due to decreased river discharge (Odebrecht et al., 2010). However, the larger lagoon system is wind forced rather than tidal driven and has subtidal circulation intervals between 3-16 days which coincide with the passage of frontal systems (Fernandes et al., 2002). This causes subtidal exchanges to be primarily driven by pressure gradients from NE or SW winds that drive seaward or landward flows respectively (Moller et al., 2001).

The area of lagoon defined as an estuary is roughly 10% of the total area (971km²) and is the southernmost portion of the lagoon (Asmus, 1997). The mean tidal amplitude experienced by the lagoon is 0.47m (Odebrecht et al., 2010). The majority of the estuarine area is shallow with 80% of the area less than depths of 1.5m. A large area of 300km² is unvegetated subtidal soft bottoms with an additional 120km² covered in seagrass beds (Seeliger and Kjerfve, 2000). These shallow conditions with a small tidal range create a good environment for seagrass beds. Marginal marshes take up an additional 70km² with artificial substrates taking up a small 0.18km² of area (Costa et al., 1997; Seeliger and Kjerfve, 2000).

1.8.2 Geologic Setting

The formation of Patos Lagoon was fueled by multiple sand barrier complex systems driven by changes of the eustatic sea level during the Quaternary (Calliari et al., 1997). When the Atlantic Ocean extended over the coastal plain during the early Pleistocene (400,000BP), the initial structures of the lagoon were formed as coastal waves and currents gradually deposited sandbars (Villwock, 1984). The following glacial period (17,000 BP) resulted in a drop in sea level to 120m below present levels. Holocene marine transgression (5,500 BP) later raised sea level 3-5m above present levels and the

subsequent regression deposited the external sand bars, dune ridges, lagoonal terraces, and beaches that now shape the landscape (Odebrecht et al., 2010). This last regression left a consistent 6m deposit of Holocene mud throughout the lagoon system (Toldo et al., 2000).

1.8.3 People and Patos Lagoon

The Patos-Mirim Lagoon system is home to 3.5 million inhabitants spanning from Porto Alegre to the north and Rio Grande to the south (Odebrecht et al., 2010). The majority of the salt marshes and seagrass beds are located within the Patos Estuary, the southern outlet of the lagoon system into the Atlantic Ocean. These coastal ecosystems and shallow embayments have proven to be essential habitat for nursing and growing near-shore fisheries in Southern Brazil and have become a large economic asset to the 170,000 people of Rio Grande who utilize the area for industrial activities, tourism, and port activities leaving it a high risk for contamination and geomorphological alternation (Tagliani et al., 2003). The increasing exploitation of this environment leaves it at risk of geomorphological alterations and anthropogenic pollution, which already have been shown to decrease and degrade the salt marsh and seagrass populations in the area (Tagliani and Asmus, 1997). With seagrasses and salt marshes both very responsive to changes in their environment it can be seen that the growing industry and population in the surrounding area could negatively impact the health of these two ecosystems.

Methods

2.1 Overview

Sediment cores of 50cm in depth were taken across three transects from salt marshes to seagrass beds or unvegetated sediments in Patos Lagoon, Brazil. Representative plant species were also collected from a given area at each sampling site. The sediments were analyzed for total carbon content as well as their bulk isotope geochemistry of $^{13}\text{C}/^{12}\text{C}$ and $^{15}\text{N}/^{14}\text{N}$. The isotopic composition and %C was also measured for the plant samples. Bulk C/N values were used with $\delta^{13}\text{C}$ and $\delta^{15}\text{N}$ to analyze the source of the organic matter by comparing them to the plant samples and preexisting values. Bulk density was used with %C to calculate average carbon density of each core. Biomass calculations for aboveground and belowground plant matter were combined with the total carbon content of the sediment to extrapolate the carbon pool of each core down to a depth of 50cm.

2.2 Field Work in Patos Lagoon

2.2.1 Sediments

A total of 15 sediment cores were collected in Patos Lagoon on August 12, 2015, August 24, 2015, and August 25, 2015. Two different custom-made corers were used to manually collect the sediment cores. The 5 cores collected on August 12th were taken using a 10cm diameter core, whereas the remaining cores were taken with a 7.5cm diameter core. The corers were constructed from a 60cm piece of plastic pipe attached to a removable top complete with handles and a valve (Figure 2.1). The valve was closed when removing cores from the ground to create a suction preventing the sediments from moving within the device. On each field date, 5 cores were taken along a transect spanning from marsh, to seagrass beds, to slightly more offshore basins. For this thesis only the 1st, 3rd, and 5th cores of each transect were studied.

Figure 2.2 shows a general site map with the location of Transects 1, 2, and 3 and their respective cores. The depths of the cores ranged from 44-60cm, but for the purposes of this thesis, only the upper 50cm of each core will be discussed. Cores were taken on foot in water depths of 0-19cm in marshes, 64.5-75cm in seagrass beds, and 87-93cm in deeper basins. Waters were relatively calm on all three field days. After the cores were collected, excess water was syphoned off and the cores were packed on either end with Styrofoam for stabilization and transported upright back to a lab at the Department of Oceanography at the Universidade Federal do Rio Grande (FURG) where they were stored at 4°C.



Figure 2.1: A) Coring device with 7.5cm diameter tube and removable top B) A sediment core in the casing with the top removed, packed with cloth and styrofoam, and caps placed on top and bottom

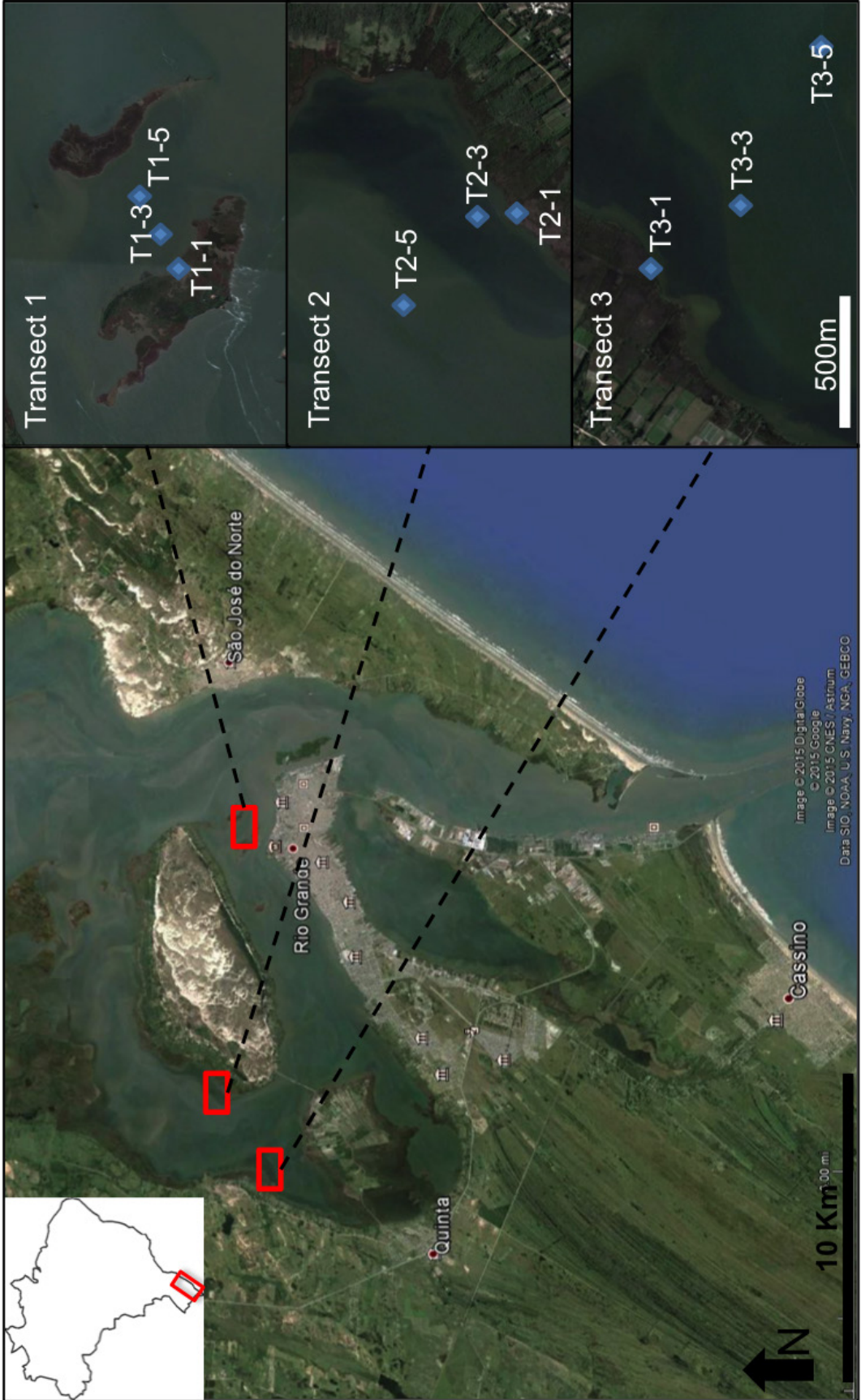


Figure 2.2: Site map of Patos Lagoon with Transects 1, 2, 3, outlined in red boxes. Inset maps show detailed image of each transect with each core location shown with a blue dot. Images taken from Google Earth, 2015.

Table 2.1 Species collected for biomass at each core site * not analyzed in this study*

Date Collected	Transect #	Core #	Core Name	Core Length (cm)	Water Depth (cm)	Location Description	Species Collected (# of samples)
8-Aug-15	1	1	T1-1	52	9	Marsh (100m from edge of platform)	<i>Spartina densiflora</i> (1), <i>Scirpus maritimus</i> (1)*, <i>Spartina alterniflora</i> (1)*
8-Aug-15	1	2	T1-2*	57	16	Edge of Marsh Platform	<i>Spartina densiflora</i> (1)*
8-Aug-15	1	3	T1-3	62	60	Tidal Flat	No vegetation
8-Aug-15	1	4	T1-4*	61	77	Tidal Flat	No vegetation
8-Aug-15	1	5	T1-5	45	87	Tidal Flat	No vegetation
24-Aug-15	2	1	T2-1	54.5	19	Marsh (100m from edge of platform)	<i>Scirpus maritimus</i> (3)
24-Aug-15	2	2	T2-2*	46.5	29.5	Edge of Marsh Platform	<i>Scirpus maritimus</i> (3)
24-Aug-15	2	3	T2-3	57.5	75	Seagrass Bed	<i>Ruppia maritima</i> (3)
24-Aug-15	2	4	T2-4*	57	84	Seagrass Bed	<i>Ruppia maritima</i> (3)
24-Aug-15	2	5	T2-5	60.5	96	Tidal Flat	No vegetation
25-Aug-15	3	1	T3-1	49	0	Edge of Marsh Platform	<i>Juncus</i> spp (3)
25-Aug-15	3	2	T3-2*	58	25.4	Edge of Marsh Platform	<i>Spartina alterniflora</i> (3)*
25-Aug-15	3	3	T3-3	44	64.5	Seagrass Bed	<i>Ruppia maritima</i> (3)
25-Aug-15	3	4	T3-4*	48.5	54	Seagrass Bed	<i>Ruppia maritima</i> (3)
25-Aug-15	3	5	T3-5	60	93	Tidal Flat	No vegetation

2.2.2 Plants

At each core site the aboveground and belowground biomasses of the representative vegetation were collected within 1-2m of the site using 15cm diameter rings (Table 2.1). One replicate of each species was sampled at core T1-1 and whole plants were sampled in triplicate at cores T2-1, T2-3, T3-1, and T3-3. The entire biomass of each plant was collected including removing the entirety of the belowground biomass from the sediment. In total 5 different species were collected, four marsh species and one seagrass species.

2.3 Sample Preparation

2.3.1 Sediments

All core casings were cut with a small circular saw and split with fishing wire. One half of the core was designated as the working half and the other as the archive half which was wrapped and then stored at 4°C in a refrigerated container. A stratigraphic log of each core was made and described using parameters, such as color from a Munsell color chart, relative grain size, root densities, and presence of shell fragments. The entirety of the working half core was subsampled at 2cm increments over the top 20cm and at 5cm increments for the lower 30cm. Each sample was removed as a slice from the core casing using a metal spatula, which was wiped clean between samples to prevent cross contamination. The exact dimensions (height, diameter, and width) of each subsection were measured to obtain the wet sediment volume.

2.3.2 Plants

Plant samples were separated into their aboveground and belowground components and washed with distilled water. They were then cut into smaller pieces and dried at 60°C for 1-2days. A dry weight of each sample (aboveground and belowground) was taken.

2.4 Inductively Coupled Plasma Atomic Optical Emission Spectrometry (ICP-OES)

The upper 36cm of core T1-3 was sampled at 1cm increments and the lower 14cm at 2cm increments. Roughly 0.5g of dry sediment were weighed out and combined with 10ml of concentrated HNO₃. This solution was added to a Teflon vessel and digested in a MARSXpress microwave. The setting used was EPA 3051, which cooks each sample at 175°C for 4.5 minutes. The vessels were then cooled and diluted to 50ml using e-pure water. This solution was filtered and then run through a Thermo Scientific iCAP 6000 Series ICP Emission Spectrometer. Measurements were taken three times in a 15 second run followed by a 45 second flush time between samples.

Stable lead concentrations (ppm) were calculated for each of samples from the Pb220.3nm wavelength. The standards used were a blank, multi-element standard (MES) 1ppm, and MES 10ppm.

2.5 Elemental Analyzer-Isotope Ratio Mass Spectrometer (EA-IRMS)

The sediment and plant samples were homogenized using a SPEX 8510 ShatterBox and a SPEX 8000 Mixer/Mill, respectively. A range of 25-100mg of sediment and 2-4mg of plant were weighed out and packed into tin cups for stable isotope analysis of carbon and nitrogen.

Samples were run through a Costech Elemental Analyzer via the Conflo III combustion interface combined with a Thermofinnigan Delta V Advantage Stable Isotope Mass Spectrometer. Data provided from these runs are micromoles of nitrogen and carbon, % nitrogen and carbon, $\delta^{15}\text{N}$, and $\delta^{13}\text{C}$. C/N molar ratios can also be calculated from these data.

2.6 Bulk Density and Carbon Density

A wet weight of each sediment sample was taken immediately after subsampling. The sediments were then dried at 60°C and a dry weight taken after 1-2 days. Samples were dried until a constant mass was achieved. These dry masses were used to calculate the dry bulk density of each sample. The volume of each sample was dependent on the depth interval of the subsample and on the diameter of the core.

$$\text{Dry Bulk Density (g/cm}^3\text{)} = (\text{Dry Weight (g)}) / (\text{Wet Sample Volume (cm}^3\text{)})$$

Bulk density and % carbon were used to calculate the carbon density of each subsection of core using methods taken from Chapter 3 of the Coastal Blue Carbon Manual (Howard et al., 2014).

$$\text{Carbon Density ((g C)/cm}^3\text{)} = \text{Bulk Density ((g)/cm}^3\text{)} * ((\% \text{ Carbon}) / 100)$$

All subsections with the same thickness were averaged. The averaged values from the different subsection widths were then averaged to obtain the overall carbon density for the depth of the core. Standard deviation values were found similarly.

2.7 Carbon Stocks

All carbon stock calculations are given in units of MgC/ha-(at some depth), the most common units when assessing carbon stocks of an ecosystem. Methods for calculating carbon in biomass and sediments were taken from Chapters 4 and 3 of the Coastal Blue Carbon Manual, respectively (Howard et al., 2014).

2.7.1 Carbon in Aboveground and Belowground Biomass

The area and mass of the dried plant samples were combined to determine biomass/area. The % carbon measurement from the IRMS was multiplied to this value to calculate the amount of carbon stored in the biomass/area. This calculation was done for both the aboveground and belowground ground portions of each sample.

$$\text{Carbon in Biomass (MgC/ha)} = (\text{Weight of Sample (g)}) / (\text{Area of Sample (cm}^2\text{)}) * ((\% \text{ Carbon}) / 100) * ((1 \text{ Mg}) / 10^6 \text{ g}) * ((10^8 \text{ cm}^2) / (1 \text{ ha}))$$

2.7.2 Sediment

The amount of carbon in each core was approximated using average carbon density and the length of the core. Most carbon stock measurements use a standard of 1m depth, but due to the limitations in this study, carbon stocks can only be assessed to a depth of 50cm.

$$\text{Sediment Carbon Stock ((Mg C)/(ha))=}$$
$$\text{Average Carbon Density ((g)/cm}^3 \text{)} * \text{Length of Core(cm)} * ((1 \text{ Mg})/10^6\text{g}) * ((10^8\text{cm}^2)/(1 \text{ ha}))$$

2.7.3 Total Carbon Stock

An estimate of the total carbon content stock per core was extrapolated by combining the carbon content for aboveground and belowground biomass with the carbon of the sediment down to the depth of the core.

$$\text{Total Carbon (MgC/hectare}_{\text{to depth of core}} \text{)} = (\text{Biomass C}_{\text{above}} + \text{Biomass C}_{\text{below}} + \text{Sediment}_{\text{to depth of core}})$$

The total carbon stock of the ecosystem was then estimated by multiplying the total carbon by the area of the ecosystem.

$$\text{Total Carbon of Ecosystem (MgC)} = \text{Total Carbon (MgC/ha}_{\text{to depth of core}} \text{)} * \text{Area of Ecosystem(ha)}$$

It is assumed that vegetation type and density is constant throughout the area. It also must be assumed that carbon burial rates and average carbon density are consistent across the ecosystem. However, these conditions are rarely observed making these measurements rough estimates of the carbon stock of the ecosystem.

Results

3.1 Plant Geochemistry

Figure 3.1 shows a biplot of $\delta^{13}\text{C}$ vs $\delta^{15}\text{N}$ for the plants analyzed in this study. Table 3.1 summarizes the average $\delta^{13}\text{C}$, $\delta^{15}\text{N}$, and C/N ratio for each plant species. Complete geochemical data for each sample can be found in Appendix 1.

The average $\delta^{13}\text{C}$ value for the *Spartina densiflora* (C_4 plant) is -14.4‰ and is the highest of any of the plants analyzed. *Ruppia maritima* (seagrass) has the second highest average at -15.7‰ and ranges in value from -13.9 to -17.6‰ . *Scirpus maritimus* and *Juncus* spp (C_3 plants) have lower averaged $\delta^{13}\text{C}$ values at -25.5‰ and -29.7‰ , respectively. The range of *Scirpus maritimus* is about 1‰ whereas the *Juncus* spp is slightly larger at roughly 2‰ . Standard deviation is under 1.5‰ for all species

The majority of $\delta^{15}\text{N}$ values for all plants are clustered from 3 to 5‰ . *Ruppia maritima* has the lowest average $\delta^{15}\text{N}$ value at 3.7‰ with a range of 1.9 to 4.6‰ . The average values of *Scirpus maritimus* and *Juncus* spp are relatively similar at 4.4‰ and 4.2‰ respectively. *Spartina densiflora* has the highest $\delta^{15}\text{N}$ value at 5.2‰ . Standard deviation is under 1‰ for all species.

Spartina densiflora and *Scirpus maritimus* have similar C/N ratios at 63.0 and 60.3, respectively. These two species also have the highest standard deviation values at 22.8 and 33.2. *Juncus* spp has a C/N ratio of 44.9 and *Ruppia maritima* has the smallest value at 16.9. The standard deviation for both of these species is below 6. C/N ratios of 4-10 typically indicate sediments derived from a microplant source (phytoplankton and benthic algae) and higher values indicate sediments derived from a macroplant (higher plants and macroalgae) source (Meyers, 1994). All species measured in this study have C/N ratios higher than the microplant range confirming that they are higher plants and would represent a macroplant source of organic matter in sediments.

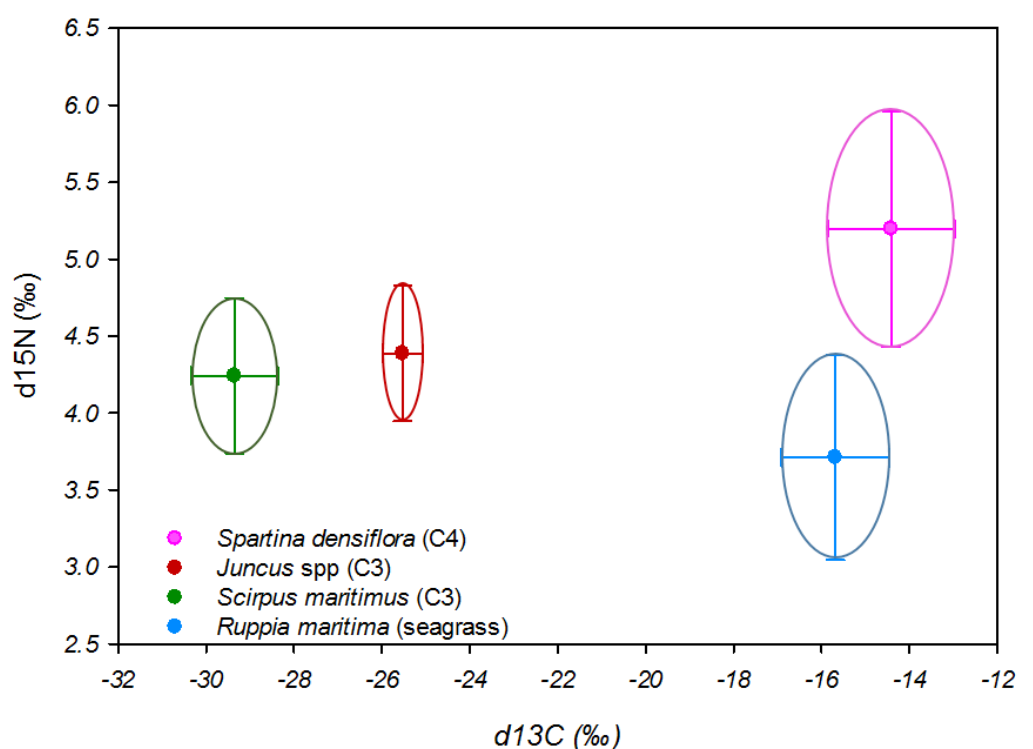


Figure 3.1: A biplot of the $\delta^{15}\text{N}$ (‰) vs $\delta^{13}\text{C}$ (‰) for all sampled plants (*Spartina densiflora*, *Juncus* spp, *Scirpus maritimus*, *Ruppia maritima*). Values plotted are averages with standard deviation.

Table 3.1: Average $\delta^{13}\text{C}$ (‰), $\delta^{15}\text{N}$ (‰), C/N ratios, and standard deviation for all plant species							
Species	$\delta^{13}\text{C}$ (‰)	$\delta^{15}\text{N}$ (‰)	C/N	Standard Deviation $\delta^{13}\text{C}$	Standard Deviation $\delta^{15}\text{N}$	Standard Deviation C/N	n=
<i>Spartina densiflora</i>	-14.4	5.2	63	1.4	0.8	22.8	2
<i>Scirpus maritimus</i>	-25.5	4.4	60.3	0.5	0.4	33.2	6
<i>Juncus</i> spp	-29.4	4.2	44.9	1	0.5	5.1	6
<i>Ruppia maritima</i>	-15.7	3.7	16.9	1.2	0.7	4.8	18

3.2 Core descriptions

3.2.1 Transect 1

Sediments collected in core T1-1 consisted of two distinct units (Figure 3.2). The lower unit was a dark greyish brown (10YR 4/2) sandy mud and extended from the bottom of the core to 14.5 cm. The upper unit was a very dark greyish brown (10YR 3/2) mud and had a dense mix of large and fine roots. The core was taken 100m from the marsh edge in vegetation that primarily consisted of *Spartina densiflora* with some dead stands of *Scirpus maritimus* (Table 2.1 summarizes data collected at each core).

The sediments preserved in core T1-3 formed two distinct units (Figure 3.3). The bottom unit was a grayish brown (10YR 5/2) sandy silt and extended from the bottom of the core to 14cm. The lower 12cm of the lower unit contained bivalve shells with some fragments as large as 5cm. The upper unit was a yellowish brown (10YR 5/4) sand that graded into the lower finer unit. Fragments of thick roots and other organic matter were found throughout the core. This core was taken in unvegetated sediments under 60cm of water.

Core T1-5 was stratigraphically similar to T1-3 and also consisted of two units (Figure 3.4). The bottom unit was a grayish brown (10YR 5/2) sandy silt and extended from the bottom of the core to 12cm. Small shell fragments were sprinkled throughout the bottom 7cm of the core. The upper unit was a brown (10YR 5/3) sand that graded into the lower, finer grained unit. Core T1-5 was also sampled in unvegetated sediments under 87cm of water.

3.2.2 Transect 2

Core T2-1 consisted of one massive unit that was a very dark brown (10YR 2/2) mud at the top of the core and transitioned to a grayish brown (10YR 5/2) silt near the bottom (Figure 3.5). Large roots were found throughout the core with fine roots dominating the upper 12cm. The core was taken roughly 100m from the marsh edge in an area dominated by sprouting *Scirpus maritimus* plants.

The sediments of core T2-3 consisted of two distinct units (Figure 3.6). The lower unit was a

brown (7.5YR 5/2) sandy silt and comprised of the lower 45cm of the core. The upper unit was a pale brown (10YR 6/3) sand and contained fine seagrass roots. Sediments were very wet and unconsolidated at the surface and became firmer downcore. The core was taken under 75cm of water and in an area populated by *Ruppia maritima*.

Sediments collected in core T2-5 were very similar to core T2-3 (Figure 3.7). The lower unit was a brown (7.5YR 5/2) sandy silt and spanned from 11cm to the bottom of the core. The upper unit was the most prominent in the upper 4cm of the core and was a pale brown (10YR 6/3) sand. Several isolated circular black patches of sediment were also present in the upper 10cm of the core. The core was taken under 89cm of water in unvegetated sediments.

3.2.3 Transect 3

The sediments of core T3-1 formed one relatively uniform unit (Figure 3.8). The core was a light yellowish brown (10YR 6/4) with some globular black patches of sediment throughout the upper 10cm. A mix of coarse and fine roots populated the upper 15cm of the core with coarse root fragments throughout. The core was comprised of a muddy matrix that became siltier with depth. Core T3-1 was collected on the marsh edge in an area dominated by *Juncus* spp.

Sediments collected in core T3-3 formed three units (Figure 3.9). The bottom unit spanned the lower 26cm of the core and was a brown (7.5YR 5/2) sandy silt. The middle unit spanned 2 to 20cm in depth and was a pale brown (10YR 6/3) sand. This layer formed a very distinct boundary with the upper unit, which was a light yellowish brown (10YR 6/4) sand and populated by fine seagrass roots. Black patches of sand were found throughout the core. This core was taken in a *Ruppia maritima* bed under 64.5cm of water.

Core T3-5 was comprised of two distinct units (Figure 3.10). The lower unit spanned from 11cm to the bottom of the core and was a brown (7.5YR 5/3) silty sand. One large shell fragment was found at 37.5cm. The upper unit was a light brown (7.5YR 6/3) and consisted of the upper 6cm of the core. The top of the core was relatively sandy and wet, with both properties decreasing downcore. This core was taken in waters 93cm deep in unvegetated sediments.

3.3 Downcore Trends

Geochemical data for all cores can be found in Appendix 2.

3.3.1 Transect 1

Shifts in some geochemical parameters correlate to the change in stratigraphy at 14.5cm in core T1-1 (Figure 3.2). The % carbon values are around 5% in the upper 12cm of the core before exponentially decreasing to values of less than 1% downcore. This shift can be attributed to a change in organic source or the decomposition of organic matter that takes place in the lower sediments. Organic carbon has been found to decrease exponentially with depth in sediments with steady state organic inputs and diagenesis (Bernier, 1980). The highest carbon content also correlates to the sediment populated by marsh roots. Bulk density triples from 0.25g/cm³ to 0.75g/cm³ downcore at the stratigraphic change from a looser mud to a denser sandy mud.

The C/N ratio of the sediments for core T1-1 generally decreases from 17 to 11 downcore. These lower values downcore could suggest that the source of sediment is derived more from a microplant source deeper in the core. The $\delta^{13}\text{C}$ values remain relatively consistent, -16 to -17‰, in the upper 14cm of the core and then decrease coinciding with the change stratigraphic composition to -18.2‰. The $\delta^{15}\text{N}$

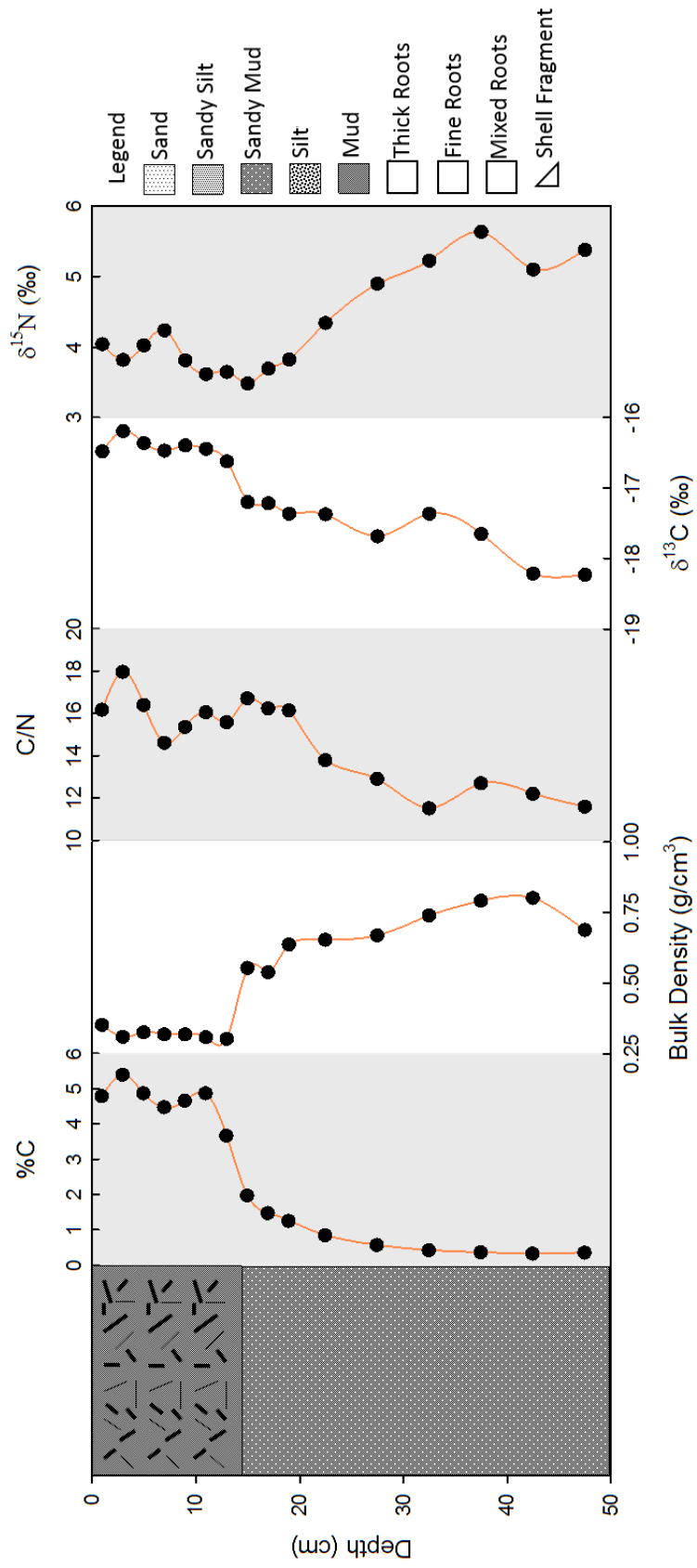


Figure 3.2: Stratigraphic log of T1-1 in leftmost panel. Geochemical data plotted against depth(cm) from left to right are %C, Bulk Density (g/cm³), C/N ratios, δ¹³C (‰), and δ¹⁵N (‰).

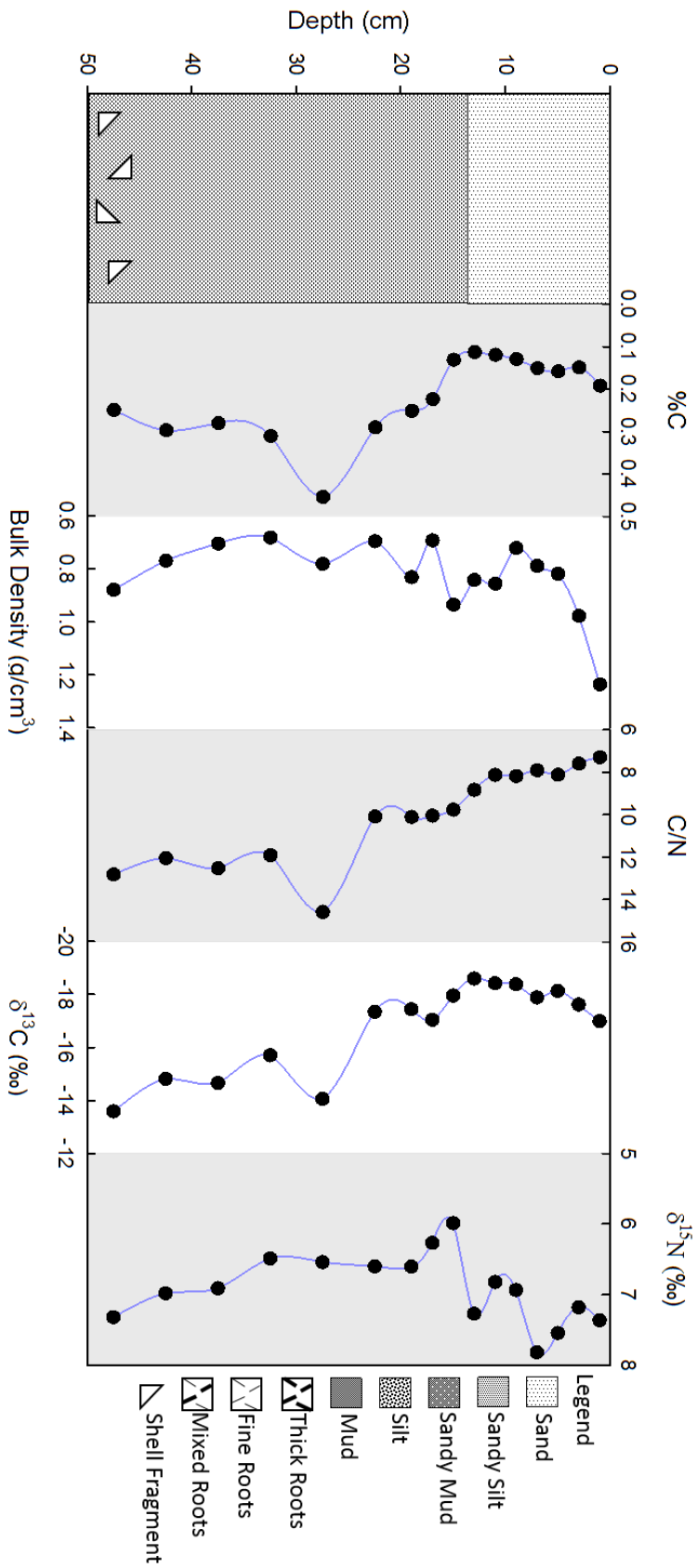


Figure 3.3: Stratigraphic log of TT1-3 in leftmost panel. Geochemical data plotted against depth(cm) from left to right are %C, Bulk Density (g/cm³), C/N Ratios, $\delta^{13}C$ (‰), and $\delta^{15}N$ (‰).

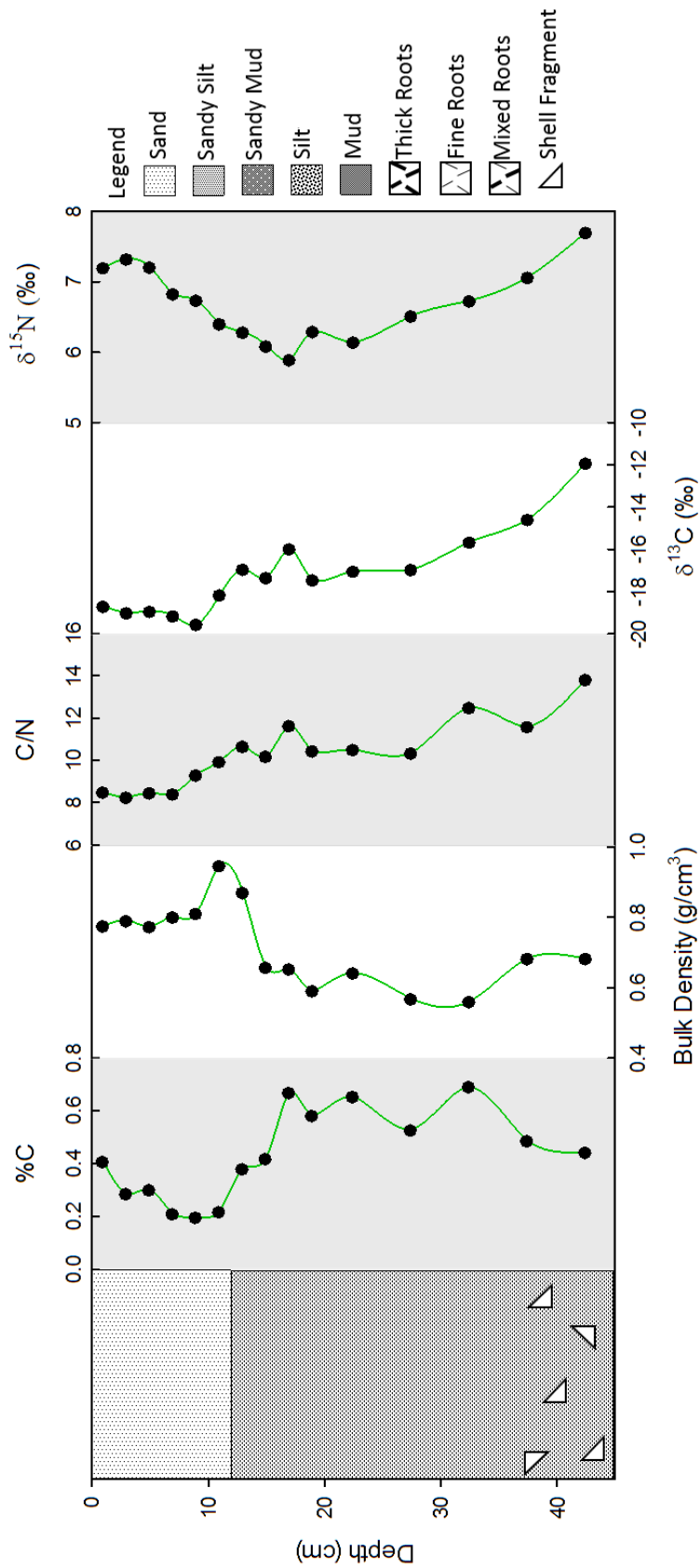


Figure 3.4: Stratigraphic log of T1-5 in leftmost panel. Geochemical data plotted against depth(cm) from left to right are %C, Bulk Density (g/cm³), C/N ratios, δ¹³C (‰), and δ¹⁵N (‰).

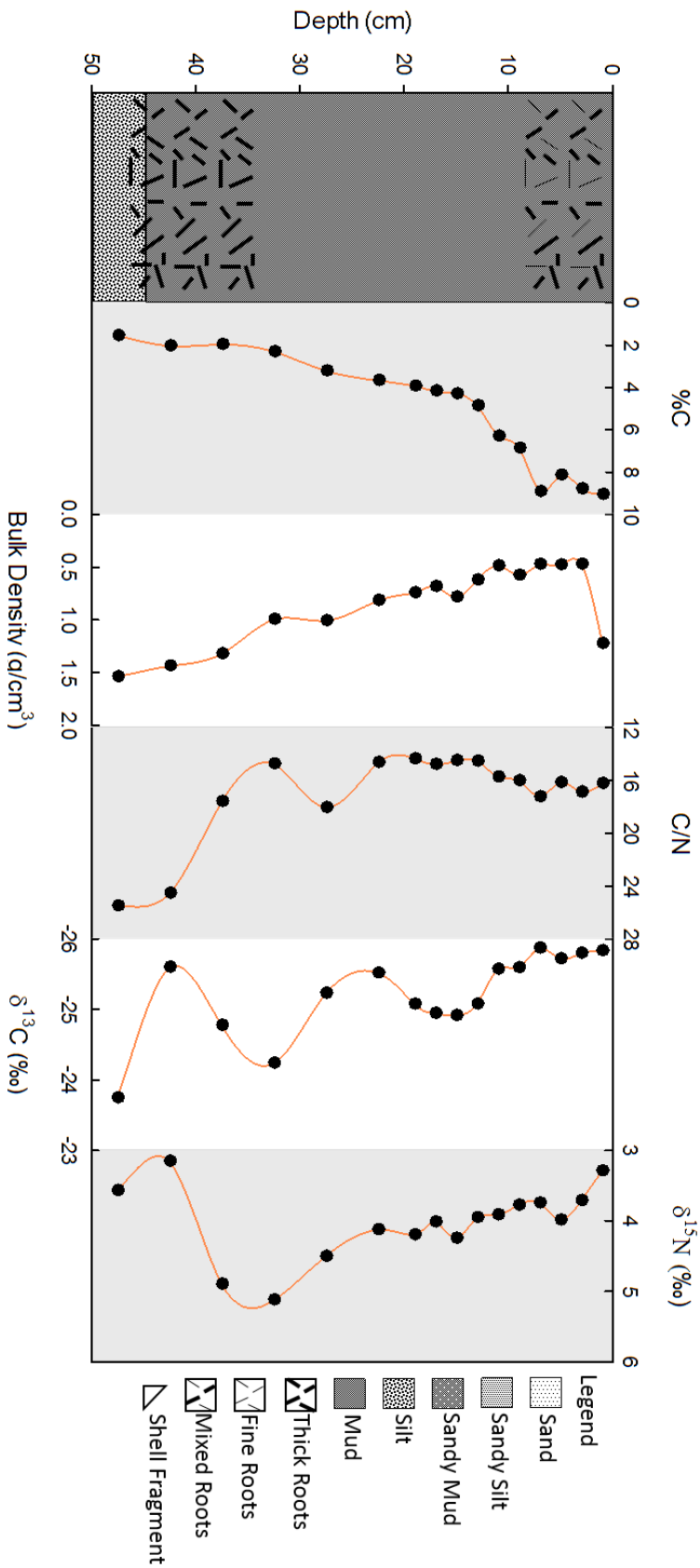


Figure 3.5: Stratigraphic log of T2-1 in leftmost panel. Geochemical data plotted against depth(cm) from left to right are %C, Bulk Density (g/cm^3), C/N ratios, $\delta^{13}\text{C}$ (‰), and $\delta^{15}\text{N}$ (‰).

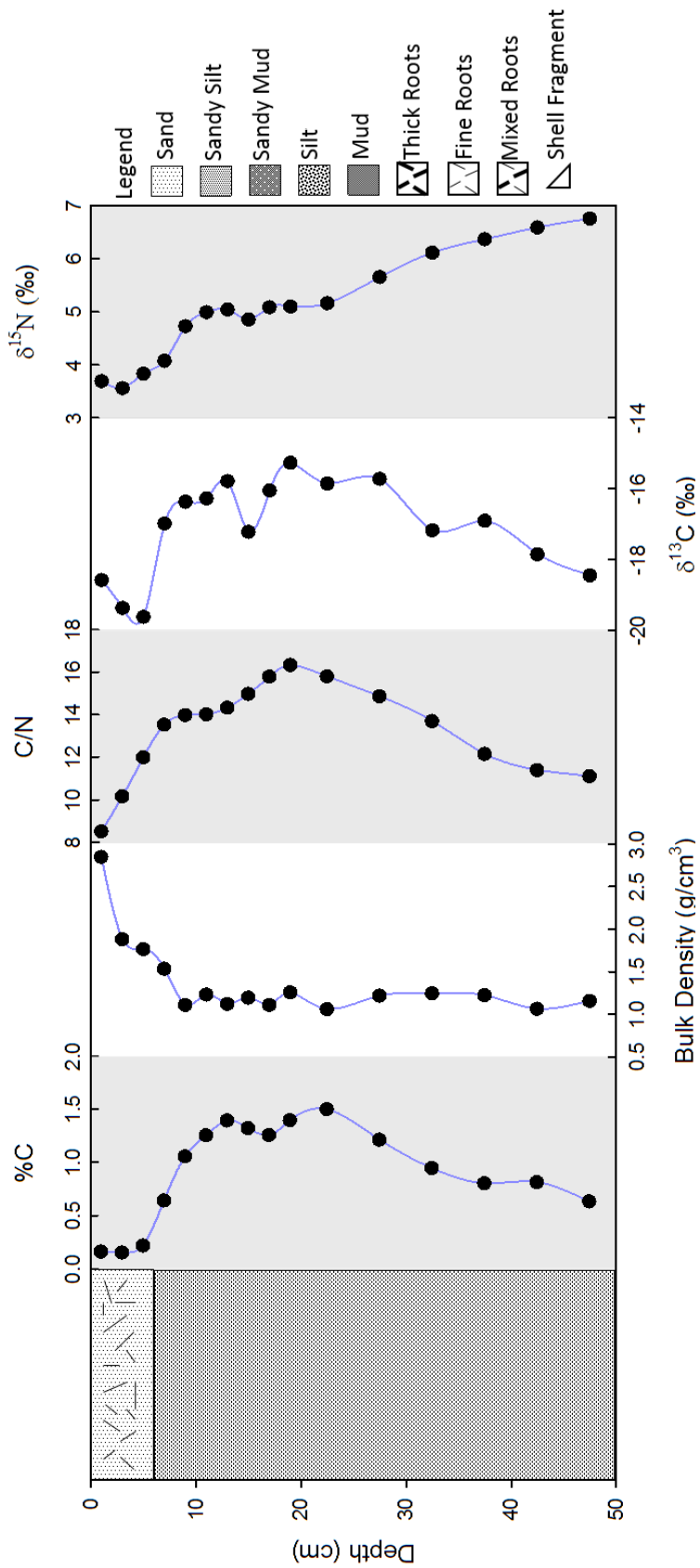


Figure 3.6: Stratigraphic log of T2-3 in leftmost panel. Geochemical data plotted against depth(cm) from left to right are %C, Bulk Density (g/cm³), C/N ratios, δ¹³C (‰), and δ¹⁵N (‰).

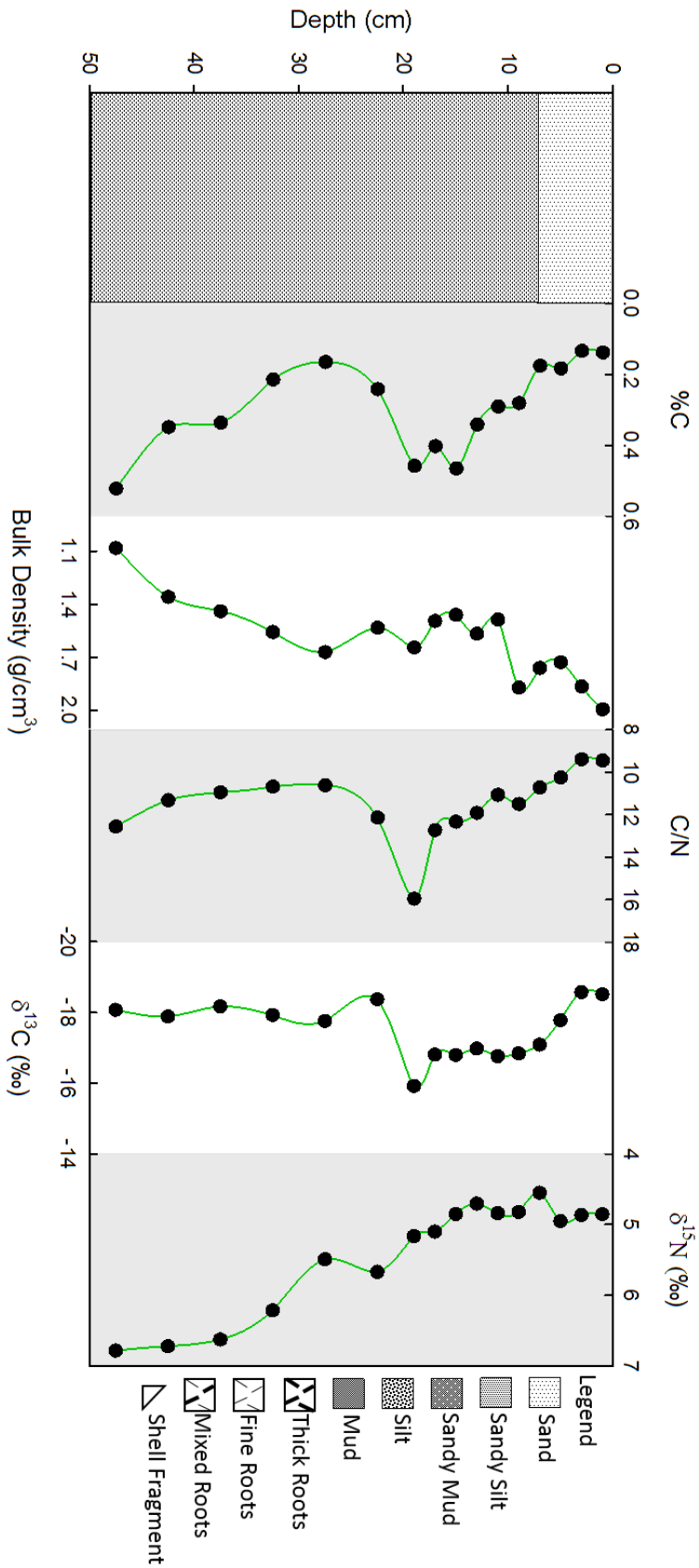


Figure 3.7: Stratigraphic log of T2-5 in leftmost panel. Geochemical data plotted against depth(cm) from left to right are %C, Bulk Density (g/cm^3), C/N ratios, $\delta^{13}\text{C}$ (‰), and $\delta^{15}\text{N}$ (‰).

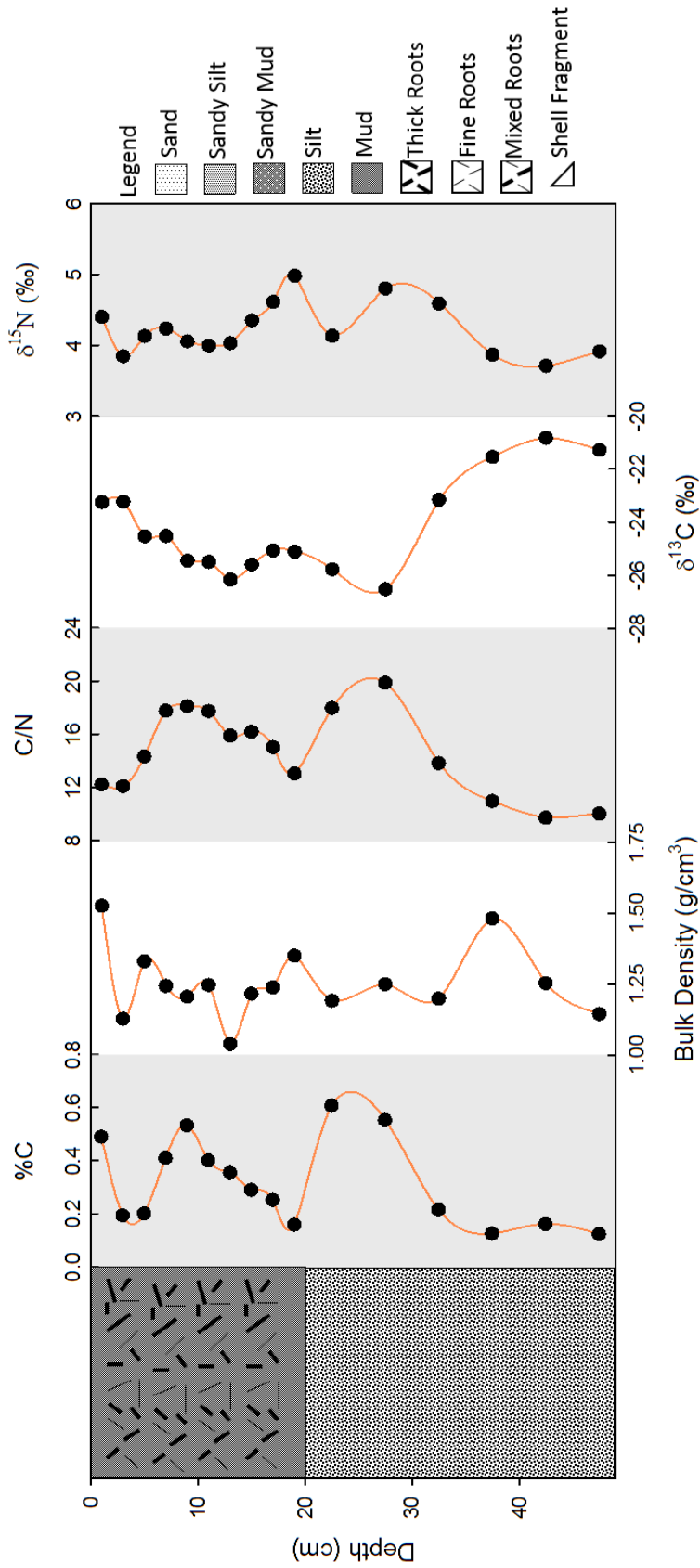
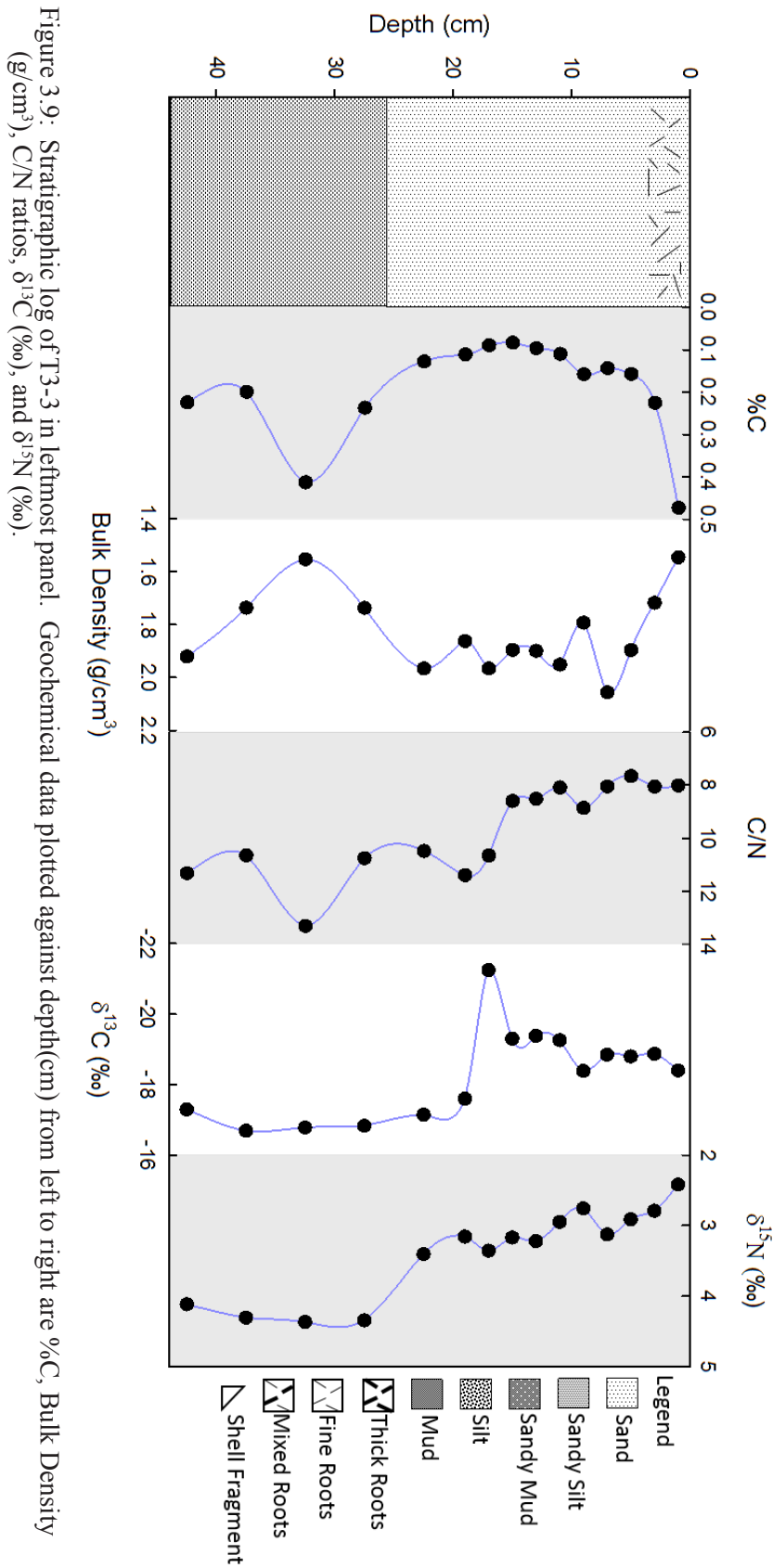


Figure 3.8: Stratigraphic log of T3-1 in leftmost panel. Geochemical data plotted against depth(cm) from left to right are %C, Bulk Density (g/cm³), C/N ratios, δ¹³C (‰), and δ¹⁵N (‰).



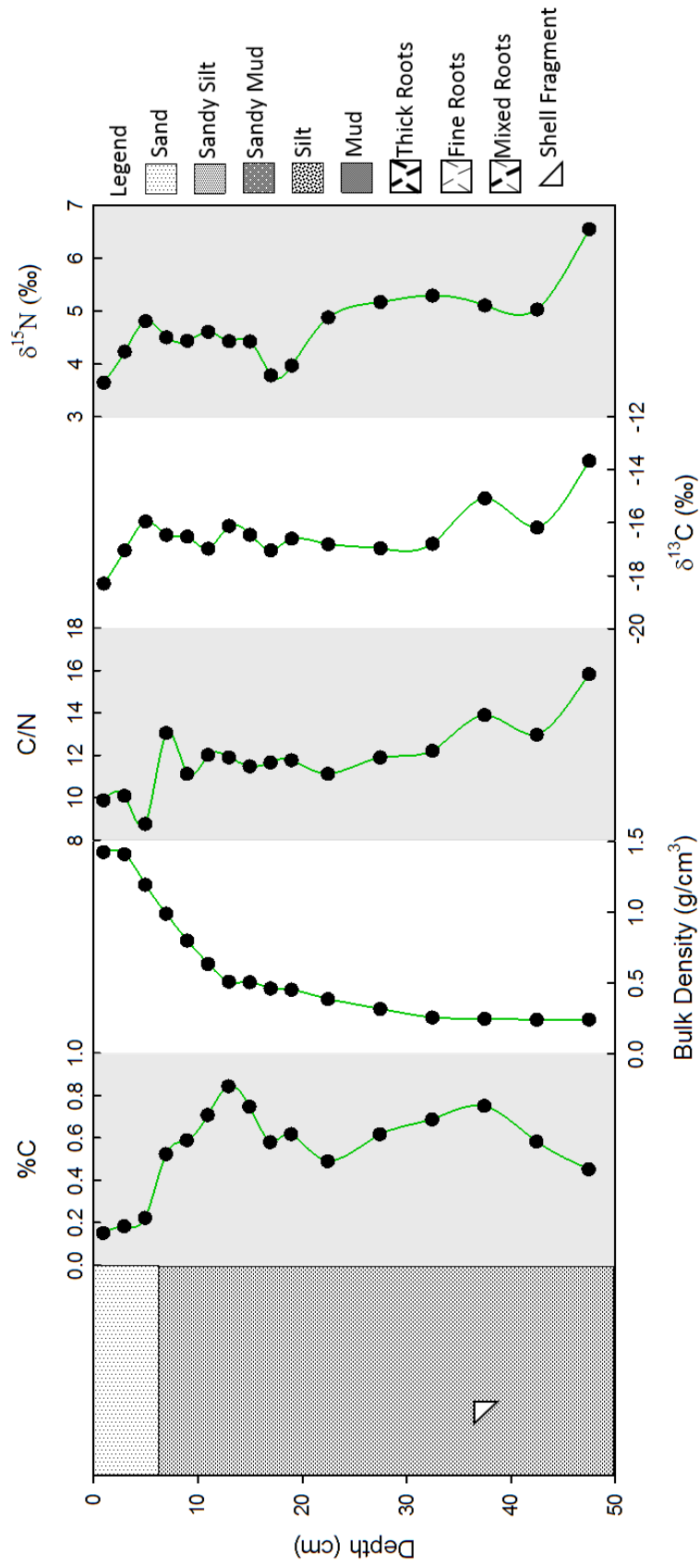


Figure 3.10: Stratigraphic log of T3-5 in leftmost panel. Geochemical data plotted against depth(cm) from left to right are %C, Bulk Density (g/cm^3), C/N ratios, $\delta^{13}\text{C}$ (‰), and $\delta^{15}\text{N}$ (‰).

values fluctuate around 4‰ over the upper 20cm and then increase to 5.5‰ downcore. Diagenesis may be responsible for these downcore shifts in $\delta^{15}\text{N}$, for it has been found to be limited to 1-2‰ in marsh sediments (Ember et al., 1987; Fogel et al., 1989).

The sedimentology and geochemical data for cores T1-3 and T1-5 are very similar (Figures 3.3 and 3.4). These similarities could suggest both cores are in a similar depositional environment. The % carbon was under 1% for all samples in both cores. However, an increase of about 0.2% occurs at around 12cm correlating with the stratigraphic change in both cores. Bulk density values are highest in the upper sand unit. The C/N ratios generally increase from 8 to 14 downcore. This suggests that sediments near the surface are derived from a microplant source such as phytoplankton, whereas a macroplant source may be more influential downcore. However, it has been found that diagenetic alteration can increase C/N ratios in sediments (Meyers, 1997). This would argue that some of the higher C/N ratios at depth for cores T1-3 and T1-5 are artificially high. The $\delta^{13}\text{C}$ values for core T1-3 have a smaller range than values for core T1-5 but show the same general trend. Values in the upper 14cm are relatively depleted in ^{13}C (-18 to -16‰) and then become enriched to about -12‰ downcore. The $\delta^{15}\text{N}$ values also have similar profiles downcore. Values are the most enriched in ^{15}N , 7‰, at the top and at the bottom of the core, with values of about 6‰ at 15cm.

3.3.2 Transect 2

Core T2-1 has geochemical similarities to T1-1 (both marsh cores) (Figure 3.5). The % carbon is the highest for any of the cores analyzed with values ranging from 1.6 to 9.1%. The % carbon profile is similar to core T1-1 with the highest values in the upper section of the core, and decreases in % carbon with depth. This suggests that carbon in T2-1 has a change in deposition and/or has undergone decomposition with increasing depth. The high % carbon values also correlates to the roots found within the upper 10cm of sediment. With the exception of the top sample, bulk density increases downcore as sediments firmed and become sandier. A similar trend is seen in core T1-1. The C/N ratios remain around 16 in the upper 40cm of the core and increase to 25.4 in the lower 10cm. These high C/N values suggest that the organic matter in the core is largely derived from macroplants and the increased values at the bottom of the core suggest either a stronger macroplant source or diagenetic alteration. The $\delta^{13}\text{C}$ values are the most depleted in ^{13}C (-26 to -25‰) in the upper 12cm of the core and then increase to -23.7‰ with depth. The $\delta^{15}\text{N}$ values remain around 4‰ in the upper 30cm and vary in the lower 20cm with values between 3 and 5‰.

Cores T2-3 and T2-5 are nearly stratigraphically identical with the exception of seagrass roots in the upper unit of core T2-3 (Figures 3.6 and 3.7). This suggests that both cores exist in a similar depositional environment. In both cores, % carbon is lower than core T2-1 with values under 2%. Both cores also show an increase in % carbon from 8 to 25cm in depth. This increase in carbon is more prominent in core T2-3 than in core T2-5. Bulk density values generally decrease downcore as the sediments become siltier with depth. C/N ratios also appear to increase in roughly the same interval as the % carbon (trend is weaker for core T2-5). Values at the top and bottom of both cores are around 8 to 10, whereas values in the middle portion of the core range from 10 to 16. This increase in both carbon and C/N ratios could suggest that increased carbon content coincides with increased inputs of macroplants. The $\delta^{13}\text{C}$ values are somewhat similar for both cores with all values falling between -16 to -10‰. In the same 8 to 25cm interval, $\delta^{13}\text{C}$ values appear to become enriched in ^{13}C in core T2-3 and to a lesser degree in core T2-5. The $\delta^{15}\text{N}$ values for both cores decrease from about 4 to 7‰ downcore.

3.3.3 Transect 3

The geochemical data for core T3-1 show relatively consistent downcore trends (Figure 3.8). The % carbon profile does not have the same pattern as the two other marsh cores from Transects 1 and 2 (T1-1 and T2-1) and had significantly less carbon overall with values ranging from 0.12 to 0.61%. Bulk density values ranged from 1.0 to 1.5g/cm³ and show no significant trend. The C/N values are above 12 for the upper 30cm of the core and then drop as low as 9.7 for the lower 20cm of the core. This shift could suggest that the sediments from the bottom of the core are from a more microplant source relative to the macroplant signal observed in upper sediments of the core. The $\delta^{13}\text{C}$ values decrease from -23.2 to -26.5‰ in the upper 30 cm and then increase to -21.3‰ in the lower 20cm. The $\delta^{15}\text{N}$ values fluctuate from 3.7 to 5.0‰.

In contrast to Transects 1 and 2 the two off shore cores, T3-3 and T3-5, are not as stratigraphically similar to each other. All % carbon values for core T3-3 are under 0.5% (Figure 3.9). The highest values of % carbon are near the surface with the exception of a high value at 40cm. Bulk density values increase with depth over the upper 10cm of the core and then range from 1.8 to 2.0 g/cm³ for the remainder of the core. C/N ratios are consistently around 8 in the upper 16cm of the core and then range from 10 to 12 for the lower depths. This increase in C/N with depth could suggest diagenetic alteration (around selective loss of N) or a change in organic source with more input from macroplants. The $\delta^{13}\text{C}$ values center around -19‰ in the upper 16cm and increase to values around -17‰ deeper in the core. The sample most depleted in ¹³C, -21.2‰, at 18cm is an outlier and occurs at the shift in value between the upper and lower sediments in the core. The $\delta^{15}\text{N}$ values decrease from 2.4 to 4.1‰ with depth.

All % carbon values for core T3-5 are under 1% (Figure 3.10). Values increase with depth in the upper 14cm of the core and then fluctuate between 0.4 to 0.8%. Bulk density decreases downcore from 1.4 to 0.24 g/cm³ with the largest change also occurring in the upper 14cm. C/N ratios range from 8.6 to 15.8 and generally increase downcore. This could be a result of diagenetic alteration or a change in organic source of increased input of macroplants with depth. The $\delta^{13}\text{C}$ values range between -18.3 to -13.6‰. The $\delta^{15}\text{N}$ values range from 3.8 to 6.5‰ and increase slightly with depth.

3.4 Carbon Density

Table 3.2 and Figure 3.11 show the average carbon density in gC/cm³ for each core. In each transect the marsh core (T1-1, T2-1, and T3-1) has the highest carbon density. Carbon density values are generally highest in Transect 2 with core T2-1 having the highest carbon density of 0.0083 gC/cm³. Transect 3 has the smallest range of carbon density between cores at 0.0026 to 0.0039 gC/cm³. Both Transects 1 and 2 have a prominent decrease between the marsh core and the remaining two cores in the transect. Standard deviation is under 0.006gC/cm³ for all cores with the exception of core T2-1 (0.0205 gC/cm³).

3.5 Sedimentary Lead Concentrations

Lead concentrations steadily in core T1-3 increase steadily from 2.1 to 4.4ppm from the bottom of the core to 15cm (Figure 3.12). Concentrations peak at 15cm and rapidly decrease to 2.2ppm at 8cm. Values stabilize and range from 2.2 to 2.7ppm for the upper 8cm of the core with the exception of an outlier at 3cm (4.9ppm). Lead concentration values for each depth can be found in Appendix 3.

Table 3.2: Average carbon density (gC/cm ³) to 50cm depth with standard deviation for each sediment core.		
Core Name	Average Carbon Density (gC/cm ³)	Standard Deviation (gC/cm ³)
T1-1	0.0083	0.0056
T1-3	0.0019	0.0007
T1-5	0.0031	0.001
T2-1	0.035	0.0205
T2-3	0.0113	0.0047
T2-5	0.0044	0.0015
T3-1	0.0039	0.0021
T3-3	0.0035	0.0016
T3-5	0.0026	0.0013

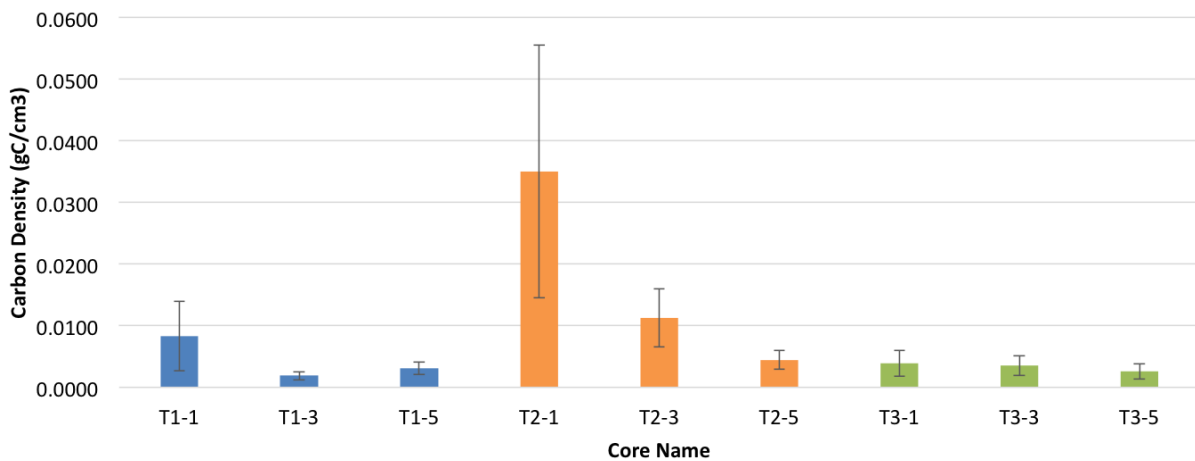


Figure 3.11: A graph of average carbon density (gC/cm³) for each core to a depth of 50cm with standard deviation. Blue bars are cores from Transect 1, orange bars are cores from Transect 2, and green bars are cores from Transect 3.

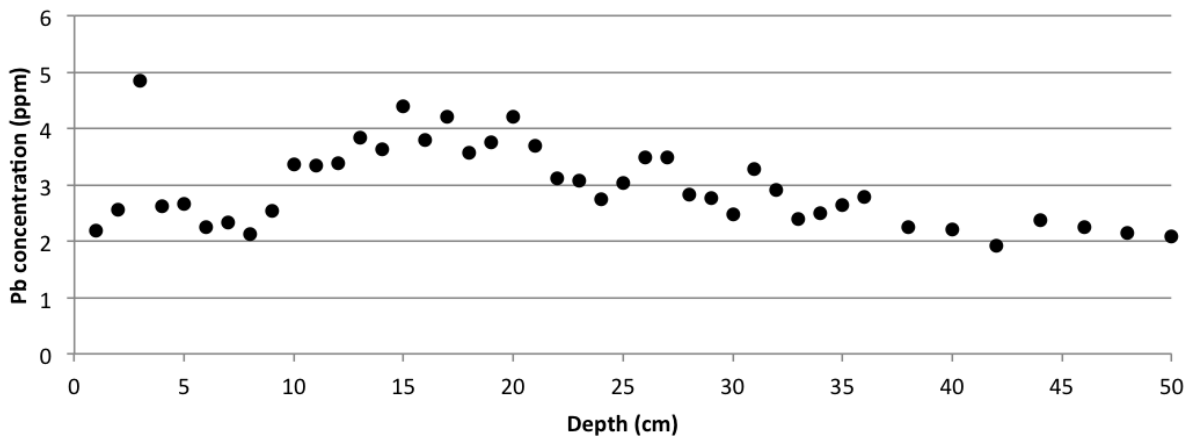


Figure 3.12: Sediment lead concentrations(ppm) plotted vs depth(cm) for core T1-3.

Discussion

4.1 Plant Biplot

The values of $\delta^{15}\text{N}$ and $\delta^{13}\text{C}$ for plants analyzed in this study are similar to those measured in previous studies (Figure 4.1). The two C_3 species (*Scirpus maritimus* and *Juncus* spp) both fall within the literature values of $\delta^{15}\text{N}$ and $\delta^{13}\text{C}$ of C_3 plants. These plants likely create the depleted $\delta^{13}\text{C}$ end member for salt marsh sediments. The one C_4 species (*Spartina densiflora*) collected falls within the literature value for $\delta^{13}\text{C}$, but is enriched by over 5‰ in ^{15}N . The seagrass species (*Ruppia maritima*) plots within the literature range of the $\delta^{15}\text{N}$ values and is depleted in ^{13}C by 6‰. No phytoplankton, macroalgae, or benthic microalgae were collected from Patos Lagoon in this study resulting in estimates for these potential carbon sources coming from literature values. Both $\delta^{15}\text{N}$ and $\delta^{13}\text{C}$ values for *Spartina densiflora* and $\delta^{13}\text{C}$ values for *Ruppia maritima* plot within macroalgae and benthic microalgae values. This makes distinguishing carbon source between C_4 plants, seagrasses, macroalgae, and benthic microalgae difficult. The enriched end member of $\delta^{13}\text{C}$ also becomes complicated to define because it could be a combination of all four of these plant groups. In future studies, macroalgae, benthic microalgae, and particulate organic matter (POM) should be sampled to better interpret the isotopic signature of potential carbon sources in the Patos Lagoon Estuary system. It is also recommended that all species should be sampled throughout the year to determine if the isotopic signature changes seasonally.

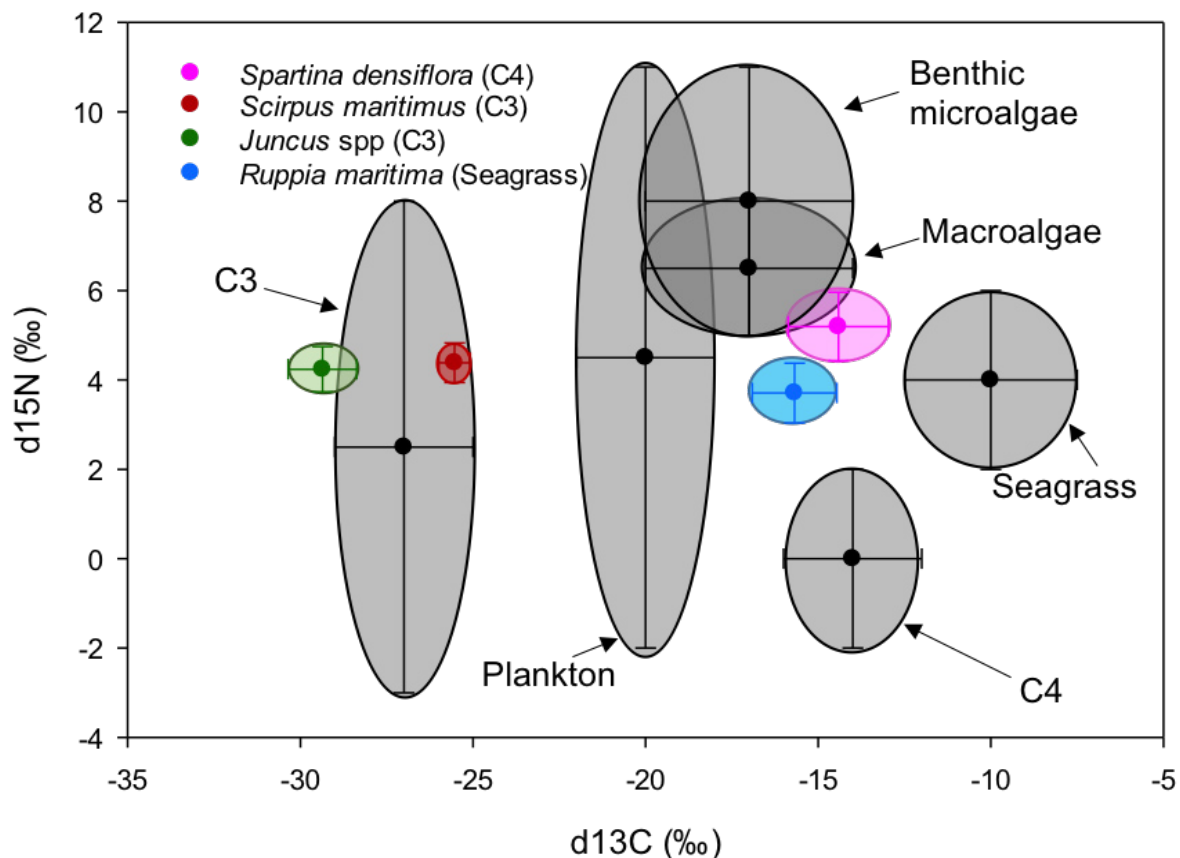


Figure 4.1: A biplot of $\delta^{13}\text{C}$ (‰) and $\delta^{15}\text{N}$ (‰) of measured isotopic values of plant samples with literature values of C_3 and C_4 plants (O'Leary, 1998; Peterson and Fry, 1987), phytoplankton (Goerike and Fry, 1994; Peterson and Fry, 1987), seagrasses (Kennedy et al., 2010 and Papadimitriou et al., 2005), macroalgae (Harris et al., 2016 (Unpublished)), and benthic microalgae (Weinstein et al., 2000).

With the exception of *Ruppia maritima*, all plants measured in this study are enriched in ^{15}N relative to the average literature values (Table 1.1). The range of measured values between samples is relatively small (3‰) compared to the range of the literature values (7‰). This suggests that the environmental conditions in Patos Lagoon result in consistently enriched $\delta^{15}\text{N}$ values for these plants. The absence of relative enrichment in ^{15}N in *Ruppia maritima* could suggest that the environmental factors causing the enrichment in $\delta^{15}\text{N}$ are largely terrestrially based. However, this is unlikely because the Patos Lagoon system is very dynamic and changes on land would most likely be reflected in the water. Alternatively, it has also been found that nitrogen fixation in seagrass beds has been shown to deplete the $\delta^{15}\text{N}$ of seagrasses regionally (Papadimitriou et al., 2005). It is possible that increased rates of nitrogen fixation in Patos Lagoon cause the seagrass beds to have depleted $\delta^{15}\text{N}$ values relative to the surrounding vegetation.

The depleted $\delta^{13}\text{C}$ values of *Ruppia maritima* relative to the literature values suggests that these seagrasses are taking up HCO_3^- or CO_2 depleted in ^{13}C or have slower photosynthetic rates. It should also be noted that literature values available originate from outside of South America and it can be expected that the isotopic signature of seagrasses could change dramatically regionally. The $\delta^{13}\text{C}$ values should be compared to regional samples and a greater study of the isotopic signature of the water in the lagoon system could explain the difference in value.

4.2 Carbon Source

Figures 4.2-4.4 are biplots of $\delta^{15}\text{N}$ vs. $\delta^{13}\text{C}$ created to evaluate the source of organic matter in the sediment cores. Downcore data (Figures 3.2-3.10) are also used to interpret changes in organic carbon source through time.

4.2.1 Transect 1

All cores have relatively enriched values of $\delta^{13}\text{C}$ with values greater than -20‰ (Figure 4.2). These enriched values suggest that C_3 plants are not a source of organic matter for the transect. The sediments of core T1-1 were collected from a *Spartina densiflora* marsh, while values plot within the range of *Ruppia maritima*. Seagrasses are an unlikely source of carbon because the tidal range is low in Patos lagoon, which would limit significant transport of seagrass plant matter onto the marsh platform. Furthermore, seagrass beds are not found in the two offshore cores. The most probable source of carbon for core T1-1 would be *Spartina densiflora*, the overlying vegetation of the core. The higher C/N ratios for this core agree with this conclusion by suggesting that the sediments are derived from a macroplant source. The fact that most of the $\delta^{13}\text{C}$ values of the sediments are depleted in ^{13}C relative to *Spartina densiflora* also suggests that phytoplankton or benthic microalgae sources could be contributing some carbon to the core. Decreasing C/N ratios and $\delta^{13}\text{C}$ values with depth imply that this core was influenced by increased levels of microplant matter with depth (Figure 3.2). The geochemistry of these sediments indicates that this core is comprised of tidal marsh sediments overlain by marsh sediments. This transition from tidal flat to marsh is most prominent from 10 to 20cm of the core where geochemical parameters change and salt marsh roots first appear.

Sediment values from both T1-3 and T1-5 do not plot in any of the isotopic ranges of the measured primary producers. This suggests that the source of carbon in these sediments is most likely controlled by a source that was not measured. The literature values of phytoplankton, macroalgae, and benthic microalgae are all enriched in $\delta^{15}\text{N}$ and depleted in $\delta^{13}\text{C}$ relative to *Ruppia maritima* and *Spartina densiflora*. These values better match the sediments suggesting that these sources are controlling the

carbon signal. The C/N ratios for both of these cores are around 10, supporting the interpretation that these sediments are more likely derived from a microplant source vs. a macroplant source. Both C/N ratios and $\delta^{13}\text{C}$ increase with depth suggesting that the source organic matter is more influenced by seagrasses or C_4 plants at depth (Figures 3.3 and 3.4). This complements the increasing % carbon with depth signifying an increased deposition of plant matter. These data indicate that sediments from cores T1-3 and T1-5 are from sparsely populated seagrass beds overlain by the tidal flat sediments seen today.

4.2.2 Transect 2

Transect 2 has a distinct signal change between the marsh and offshore cores (Figure 4.3). Most of the sediment samples from T2-1 plot near or in the range of *Scirpus maritimus*. This is consistent with marsh vegetation, which was also dominated by *Scirpus maritimus*. Coupled with high C/N ratios (Figure 3.5), this suggests that the sediments from this core are entirely based from vascular C_3 plants.

Similar to Transect 1, the sediments from the two offshore cores plot largely outside of the measured plant ranges suggesting that macroalgae, phytoplankton, and benthic microalgae could be large contributors of organic matter. However, $\delta^{13}\text{C}$ values are more enriched in ^{13}C in the middle portion of the cores suggesting that *Ruppia maritima* also could be a source of organic matter for that interval (Figures 3.6 and 3.7). Increased % carbon and C/N ratios in this same interval further suggest that seagrasses are also significant source of carbon. The % carbon values in core T2-3 are higher than in core T2-5 agreeing with the fact that seagrasses were seen at core T2-3 and not core T2-5.

4.2.3 Transect 3

Transect 3 has very low % carbon and the most variable $\delta^{13}\text{C}$ values for a marsh core (Figure 4.4). Core T3-1 has $\delta^{13}\text{C}$ values ranging between *Scirpus maritimus* and the literature values for benthic macroalgae particularly in the lower 15cm. This suggests that the carbon source in these sediments is a mix of C_3 plants and benthic microalgae. These intermediate $\delta^{13}\text{C}$ values could also represent mix of C_3 and C_4 marsh plants. *Spartina alterniflora*, a C_4 marsh plant, was seen on the marsh and can be expected to have similar $\delta^{13}\text{C}$ values to *Spartina densiflora* (-14‰). This mix of C_3 , C_4 , and benthic microalgae could also explain why sediments do not reflect the depleted $\delta^{13}\text{C}$ values of *Juncus* spp, which was the dominant vegetation found on the marsh surface. The C/N signal in the upper 30cm of the core is high and represents a macroplant source, suggesting that benthic microalgae are most likely not the source of enrichment in ^{13}C (Figure 3.8). In the deeper parts of the core, decreasing C/N ratios coupled with increasing $\delta^{13}\text{C}$ values show that sediments are derived from a microplant source, such as phytoplankton or benthic microalgae. This infers that tidal sediments dominate this lower part of core T3-1, which are overlain by marsh sediments.

The remaining offshore cores are enriched in $\delta^{13}\text{C}$ relative to the marsh core signifying a seagrass or phytoplankton source. Unlike Transects 1 and 2, the two offshore cores have isotopically different signals. Core T3-5 has a more enriched $\delta^{13}\text{C}$ signal than T3-3 suggesting that seagrasses are the dominant carbon source. This is in direct opposition with vegetation observed at these two sites, seagrasses at core T3-3 and no vegetation at core T3-5. However, % carbon and C/N ratios are also higher in core T3-5, especially with depth, which implies that seagrasses could have populated the sediments at this site in the past (Figure 3.10). The lower $\delta^{13}\text{C}$ and C/N ratios observed in core T3-3 suggest that the sediments have largely been dominated by a planktonic signal (Figure 3.9). These variable data at these two offshore cores suggest that seagrass beds at this site are ephemeral in nature.

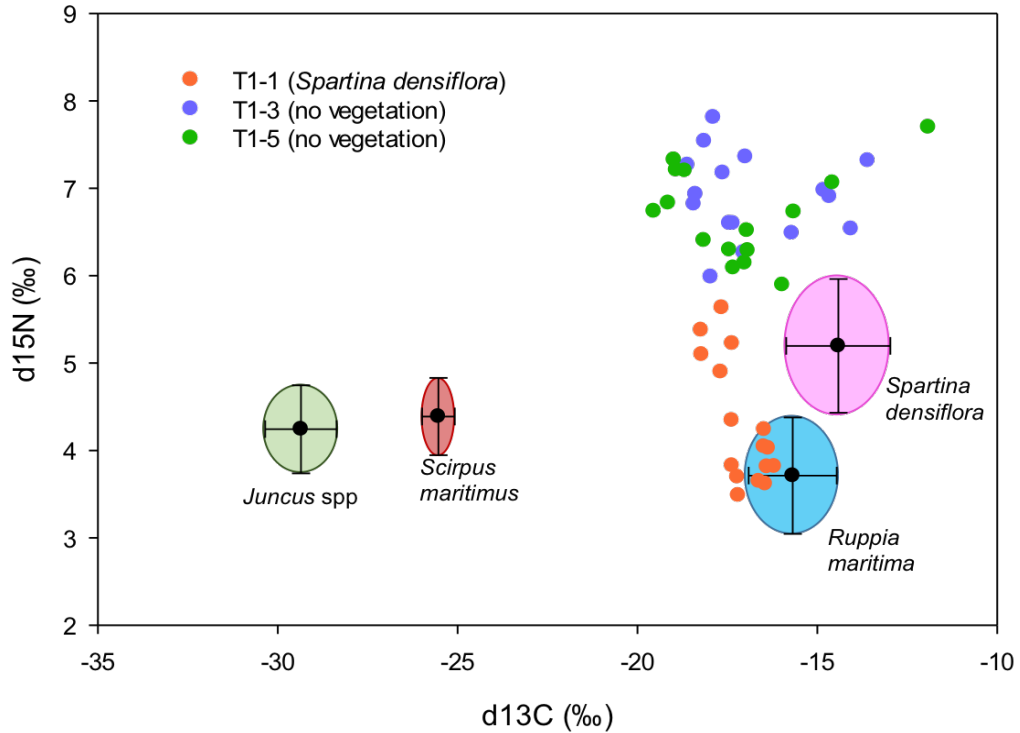


Figure 4.2: A biplot of $\delta^{13}\text{C}$ (‰) and $\delta^{15}\text{N}$ (‰) showing sediment samples from Transect 1 plotted as dots. Average isotopic values of vegetation samples are plotted with standard deviation as ovals.

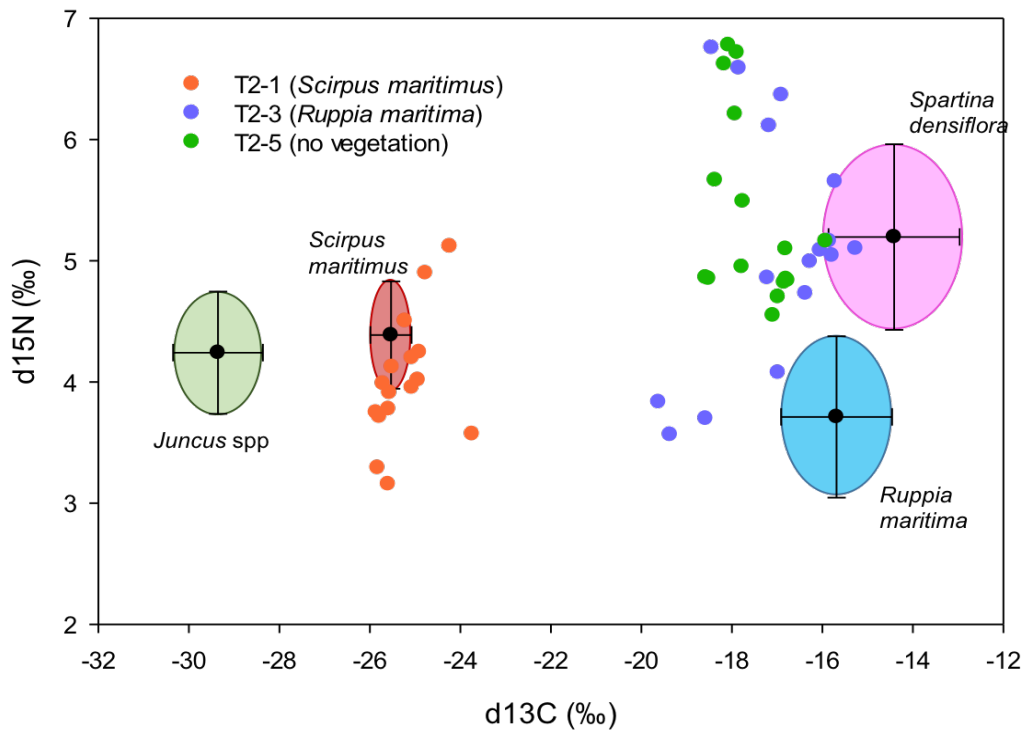


Figure 4.3: A biplot of $\delta^{13}\text{C}$ (‰) and $\delta^{15}\text{N}$ (‰) showing sediment samples from Transect 2 plotted as dots. Average isotopic values of vegetation samples are plotted with standard deviation as ovals.

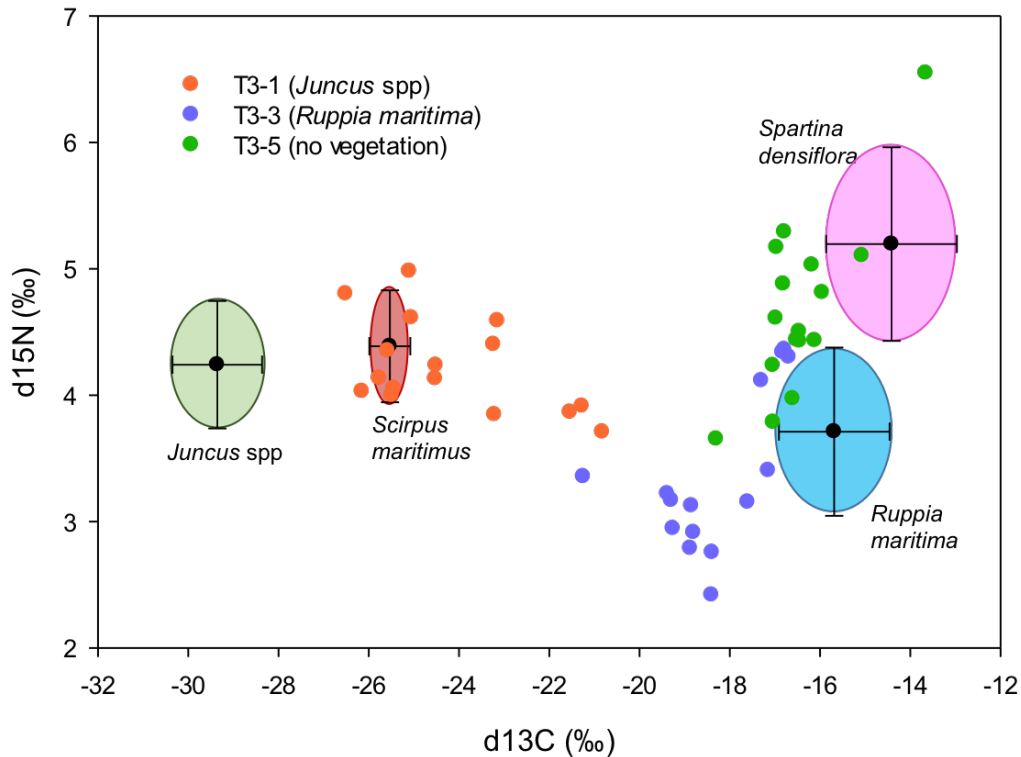


Figure 4.4: A biplot of $\delta^{13}\text{C}$ (‰) and $\delta^{15}\text{N}$ (‰) showing sediment samples from Transect 3 plotted as dots. Average isotopic values of vegetation samples are plotted with standard deviation as ovals.

4.3 Enriched $\delta^{15}\text{N}$

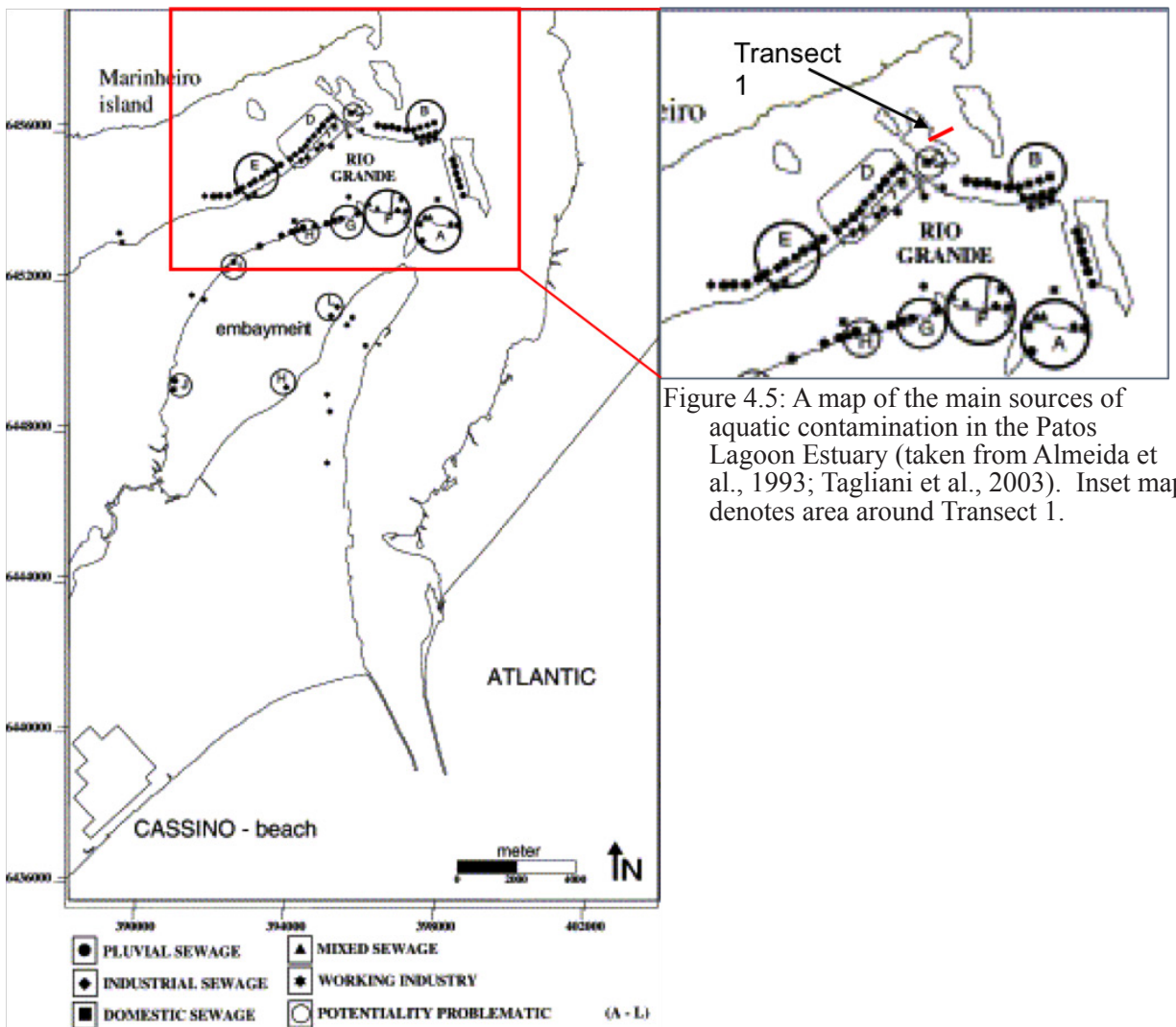
As previously discussed, many of the vegetation samples are enriched in $\delta^{15}\text{N}$ relative to the average literature values. Furthermore, most sediment samples from cores T1-3 and T1-5 and some samples from cores T2-3 and T2-5 are enriched relative to the plant samples. All of the enriched samples are found in submerged sediments suggesting that the source of enriched $\delta^{15}\text{N}$ is related to an aquatic process. All offshore sediment cores show increasing $\delta^{15}\text{N}$ values with depth, with the exceptions of cores T1-3 and T1-5 which have depleted values in the middle of the core that increase both with depth and towards the surface (Figures 3.3 and 3.4). It is possible that these sediments are enriched in ^{15}N by another source of organic matter that was not measured in Patos Lagoon, such as POM or macroalgae. However, this fails to address the enriched $\delta^{15}\text{N}$ plant values and ignores other sources of enrichment such as denitrification and anthropogenic waste.

Fractionation from denitrification ranges from -40 to -5‰ (Sharp, 2007). When denitrification occurs in anoxic sediments, depleted N_2 is released, which enriches the remaining nitrate in the sediments. This enriched nitrate is assimilated by plants causing increased $\delta^{15}\text{N}$ values of plant matter and sediments. This process of higher denitrification rates has been linked to $\delta^{15}\text{N}$ signals in seagrass beds (Papadimitriou et al., 2005). Increased levels of denitrification in Patos Lagoon could be controlling the enriched values of $\delta^{15}\text{N}$ seen in plant samples, but does not explain why some sediments are enriched relative to the plants.

Increasing $\delta^{15}\text{N}$ values of sediments towards the surface of cores T1-3 and T1-5 are likely a result of increasing amounts of anthropogenic waste entering the Patos Lagoon Estuary system. Human and animal waste have been shown to have enriched $\delta^{15}\text{N}$ values of 10-20‰ (Kreitler and Browning, 1983).

This is significantly higher than $\delta^{15}\text{N}$ values of measured plants and might explain why the sediments from these two cores are more enriched (Fry, 1991). Rio Grande is a populated area with large port industries such as food packing, fertilizer factories, oil refineries, chemical manufacturing and shipyards, all of which generate waste (Niencheski et al., 2014). Additionally, the majority of the sewage effluent from the city is untreated and dumped into the estuary (Baumgarten et al., 2001). One study found that the level of hydrocarbon pollution in the estuary was moderate to high (Medeiros et al., 2005).

The main sources of anthropogenic contamination around Rio Grande are shown on Figure 4.5. Transect 1 can be seen near outlets for pluvial, industrial, domestic, and mixed sewage all dumping into the estuary. These different wastes could all be contributors to the enriched $\delta^{15}\text{N}$ signal of the sediments at cores T1-3 and T1-5. The increasing $\delta^{15}\text{N}$ trend towards the surface in both cores could be a reflection of how anthropogenic pollution has increased with time. There are no data available for the area surrounding Transects 2 and 3, but the absence of this pattern in all other cores suggests that anthropogenic pollution is not a contributing factor at other sites. Currents near the mouth of the Patos Lagoon Estuary are primarily southward and are much weaker in shallower areas (Medeiros et al., 2005; Moller et al., 2001). This circulation pattern would move pollutants from Rio Grande out to the Atlantic Ocean and away from Transects 2 and 3.



High primary production rates are also a process that could result in an increased $\delta^{15}\text{N}$ signal in plants. Higher rates of primary productivity decreases the available nitrate pool forcing plants to incorporate higher concentrations of ^{15}N and increasing $\delta^{15}\text{N}$ of plants by 1 to 2‰. The enriched $\delta^{15}\text{N}$ values in the sediments of cores T1-3 and T1-5 is derived primarily from phytoplankton and may be explained by higher rates of primary productivity combined with the uptake of isotopically enriched nitrogen. Transects 2 and 3 both had seagrass beds and could have been controlled by primary production. Transect 3 has higher $\delta^{15}\text{N}$ values than Transect 2 suggesting that rates of primary production are higher at Transect 3. While this might explain why baseline levels of $\delta^{15}\text{N}$ are higher at Transect 3 vs. Transect 2, it does not explain why $\delta^{15}\text{N}$ values enrich downcore for all of the offshore sites.

All of the sediment cores, with the exception of T3-1, have $\delta^{15}\text{N}$ values enriching downcore at some depth. This can partially be explained by diagenetic decomposition. During the decomposition of organic matter ^{14}N is broken down at a faster rate than ^{15}N causing $\delta^{15}\text{N}$ to increase with depth as more organic matter is decomposed. It has been found that denitrification and decomposition have both been shown to increase $\delta^{15}\text{N}$ of soils at depth (Hobbie and Ouimette, 2009). It is possible that both of these processes are occurring in conjunction at some of the core sites resulting in this enrichment pattern.

4.4 Carbon Sequestration

4.4.1 The History of Leaded Gasoline as an Age Model

The use of leaded gasoline started in earnest in the 1900-1920s with the popularization of internal combustion engine and peaked in the 70s. It can be inferred from the lead concentrations in T1-3 that the increasing trend in the lower section of the core represents the increasing use of leaded gasoline in the early to mid twentieth century. The relatively abrupt decline in concentrations from 15 to 10cm most likely reflects the discontinuation of the use of leaded gasoline in Brazil, which was finally phased out in the early 90s (Lovei, 1998). This transition suggests that the peak in lead concentrations at 15cm denotes the highest leaded gasoline use in 1970 creating a sedimentation rate of 0.3cm/yr.

This sedimentation rate agrees relatively well with rates found by Toldo et al. (2000) and Niencheski et al. (2014) of 0.35-0.83cm/yr and 0.3-0.34cm/yr respectively. The study site used by Niencheski et al. (2014) was located within 200m of core T1-3 suggesting that 0.3cm/yr is a reasonable sedimentation rate for the submerged cores collected at Transect 1 and perhaps at Transects 2 and 3. Sedimentation rates in previous studies were found using ^{210}Pb and ^{137}Cs dating methods. However, these methods can be very expensive and the similarity of results between these methods and the ones used in this study suggest that the history of leaded gasoline in Brazil could be used as a cheap alternative for calculating short-term sedimentation rates in Patos Lagoon.

The sedimentation rate calculation is built on the assumption that sedimentation is consistent throughout the core and that there is no loss of the record. It is also assumed that the lead record in Brazil follows trend with global processes.

4.4.2 Carbon Burial Rates

A preliminary carbon burial rate for the shallow estuarine settings in Patos Lagoon can be calculated using the sedimentation rate from core T1-3 and the average carbon density for each core.

$$\text{Burial Rate}(\text{gC}/\text{m}^2/\text{yr}) = \text{sedimentation rate}(\text{m}/\text{yr}) * \text{average carbon density}(\text{gC}/\text{m}^3)$$

Due to similar environmental settings and geochemical data, the same sedimentation rate of

0.3cm/yr is assumed for all offshore cores (Figure 4.6). Carbon burial rates are not calculated for the cores taken in marshes because accumulation rates are often dramatically different from rates calculated off the marsh platform. Carbon burial rates range from 5 to 34gC/m²/yr (Table 4.1). Cores from Transect 2 have the highest burial rates followed by Transect 3, and Transect 1 respectively. This is expected because Transect 2 also has higher carbon density values. This suggests that carbon sequestration is highest along Transect 2. Similarly the two seagrass cores have higher carbon densities than the accompanying unvegetated core in the same transect implying that seagrasses likely directly contribute to higher rates of carbon burial.

Core	Vegetation Type	Carbon Density (gC/cm ³)	Sedimentation Rate (cm/yr)	Burial Rate (gC/m ² /yr)	Standard Deviation (gC/m ² /yr)
T1-3	none	0.0019	0.3	6	2.1
T1-5	none	0.0031	0.3	9	3
T2-3	<i>Ruppia maritima</i>	0.0113	0.3	34	14.2
T2-5	none	0.0044	0.3	13	4.6
T3-3	<i>Ruppia maritima</i>	0.0035	0.3	11	4.9
T3-5	none	0.0026	0.3	8	3.8

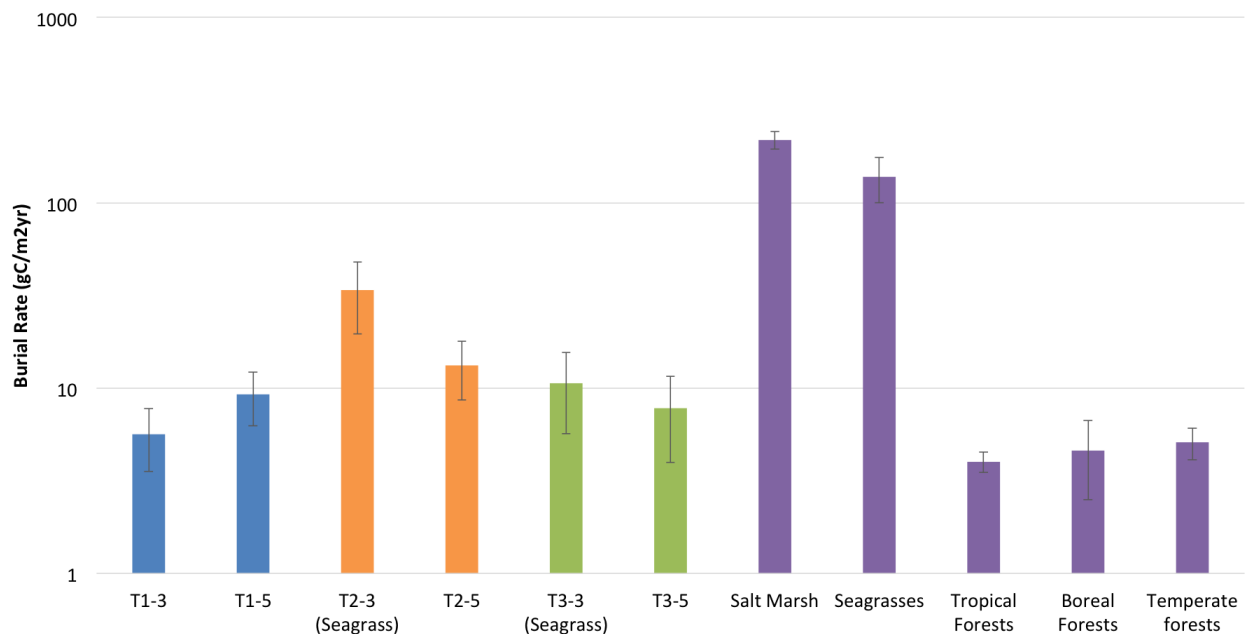


Figure 4.6: Carbon burial rates (gC/m²/yr) from offshore cores of Transects 1-3. Literature values of burial rates of different ecosystems taken from Mcleod et al., 2011. Note log scale.

When compared to the carbon burial rates of ecosystems compiled in Mcleod et al. (2011) all of the cores have higher rates than the three terrestrial ecosystems (tropical, boreal, and temperate rainforests). However, burial rates of seagrasses and marshes from the literature are larger than the values measured in this study by several orders of magnitude. This difference suggests that the seagrass beds in Patos Lagoon are less productive compared to previous studies. It is possible that the burial rates for this study are underestimated due to the simplified sedimentation rate used in this study. It should be noted that even the sites without vegetation have higher carbon burial rates than terrestrial ecosystems, which implies that these environments might be bigger carbon sinks than previously thought.

When the burial rates for the seagrass sites are compared to the biomass carbon stock of *Ruppia maritima* (discussed in section 4.5 and Table 4.2) it is found that up to 25 to 80% of the seagrass biomass is buried each year. This is assuming that all carbon in the seagrass cores is from the seagrasses themselves. Given that the isotopic data suggest that carbon buried in these sediments is most likely from a mix of sources, these values are most likely large overestimates.

4.5 Carbon Stocks

4.5.1 Biomass

Average carbon content for above and belowground biomass are given for all plant species in Table 4.2 and Figure 4.7. The raw data used to calculate carbon content can be found in Appendix 1. Total carbon content for the marsh plants ranged from 46 to 77 MgC/ha. These values are higher than carbon content values calculated for similar species, 22-24MgC/ha, for *Spartina* spp and *Juncus* spp (Elsley-Quirk et al., 2011). This indicates that primary productivity in marshes in Patos Lagoon is higher than values observed in Delaware. The % belowground biomass ranges from 39 to 87%. Belowground biomass in marshes normally constitutes 65-95% of the total living biomass carbon stock (Elsley-Quirk et al., 2011). The *Spartina densiflora* and *Scirpus maritimus* samples fall within this range (64 and 87%, respectively), but *Juncus* spp falls below at 39%. The lower value for *Juncus* spp can be explained by the fact that high marsh plants have been found to store more carbon in aboveground biomass (Howard et al., 2014). *Juncus* spp is usually categorized as a high marsh plant, which might explain its smaller % belowground biomass. It is also probable that these values are underestimates due to sampling error. Sampling of the belowground biomass was limited to the area of a 15cm diameter sampler, which would likely fail to remove the entirety of the belowground biomass.

The total carbon stock for seagrasses approximates 0.42MgC/ha. This is below the average carbon stock for seagrasses in the South Atlantic, 1.06 (+/-) 0.51 MgC/ha, and well below the global average of 2.52 (+/-) 0.48 MgC/ha (Fourqurean et al., 2012; Howard et al., 2014). Additionally, only 39% of the carbon is stored in the belowground biomass of these seagrass samples. This is below the value of 67%, which is normally observed for seagrasses (Fourqurean et al., 2012). This difference indicates that the seagrasses sampled in Patos Lagoon store less carbon than observed in other areas. However, it is possible that these values are underestimates because samples were collected in the winter and not at the peak of productivity in the summer months.

Table 4.2 Carbon content for all plant species (MgC/ha)						
Species	Total Carbon (MgC/ha)	Above-ground (MgC/ha)	Below-ground Carbon (MgC/ha)	Above-ground Standard Deviation (MgC/ha)	Below-ground Standard Deviation (MgC/ha)	% Below-ground
<i>Spartina densiflora</i>	70	25	44	-	-	64
<i>Scirpus maritimus</i>	46	6	40	2	25	87
<i>Juncus spp</i>	77	48	30	26	39	39
<i>Ruppia maritima</i>	0.42	0.26	0.16	0.03	0.04	39

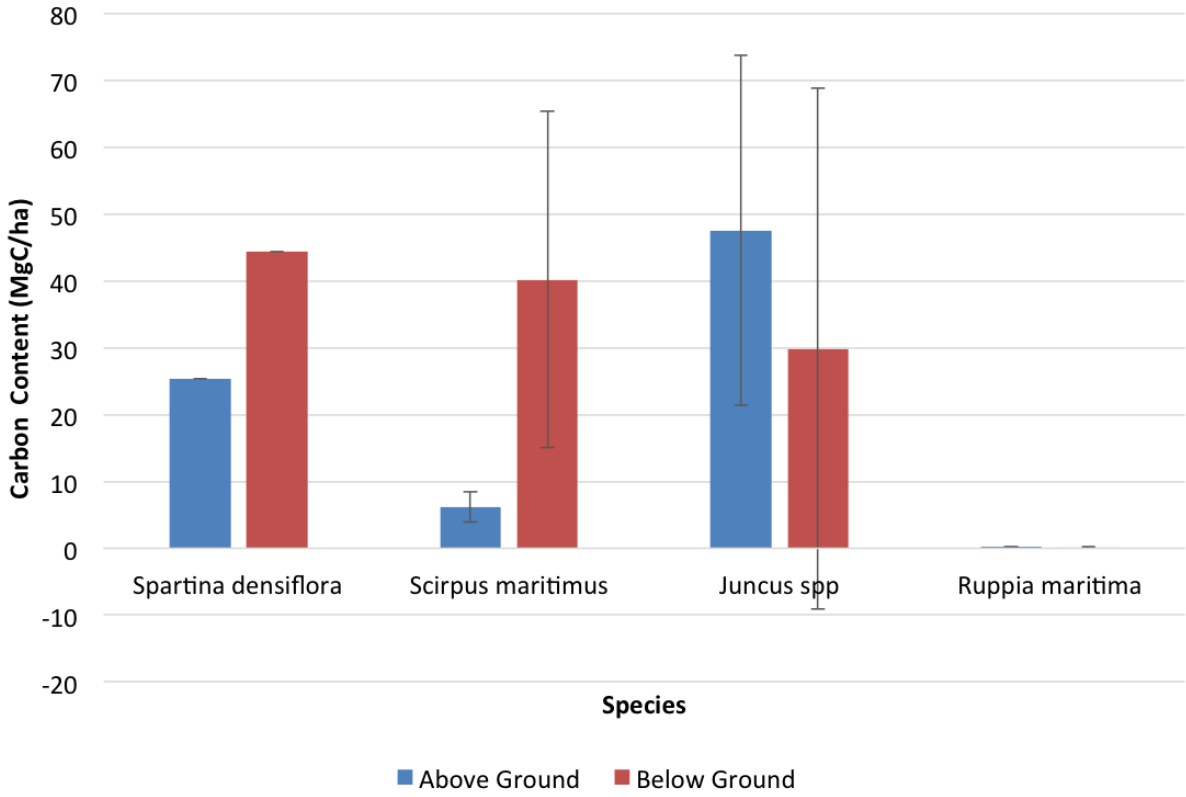


Figure 4.7: Average aboveground and belowground biomass (MgC/ha) for each species plotted with standard deviation.

4.5.2 Sediments

Table 4.3 summarizes the total organic carbon stocks from the sediments of each core. All transects show a decrease in sediment carbon stock from marsh to seagrass bed to unvegetated sediments. The marsh cores have the highest range with values from 20 to 175MgC/ha. These values demonstrate that the marshes in the area sequester highly variable amounts of carbon making it difficult to use these values to extrapolate over large areas. These variable carbon stocks could be due to the type of vegetation and also changing environmental conditions from site to site. Further research into marsh productivity and type in Patos Lagoon and how they relate to carbon productivity and sequestration would be a good direction for future work. Average sediment carbon stocks in marshes to a depth of 1m is 255MgC/ha (Howard et al., 2014). While the cores in this study were only half this length and cannot be directly compared, it should be noted that the values from Patos Lagoon fall within about an order of magnitude of global averages. This suggests that the carbon content of these cores is similar to values measured elsewhere.

The sediments in seagrass cores have a smaller range of carbon stored at 18 to 56MgC/ha. This is also comparable to the global average of seagrass sediments at 1m of 108MgC/ha (Howard et al., 2014). Most interestingly, the cores with no vegetation have values that are similar to seagrass beds with a range of 6 to 22MgC/ha. These shallow sediments may have once been occupied by seagrasses or may also collect and preserve other sources of carbon. Regardless, they appear to be just as good at storing carbon as seagrass beds. This demonstrates that not all carbon sequestration in these ecosystems comes from organic matter deposited in situ.

Core	Species	Sediment (MgC/ha)	Aboveground (MgC/ha)	Belowground (MgC/ha)	Total carbon stock (MgC/ha)
T1-1 (Marsh)	<i>Spartina densiflora</i>	41	25	44	111
T1-3	none	9	-	-	9
T1-5	none	15	-	-	15
T2-1 (Marsh)	<i>Scirpus maritimus</i>	175	6	40	221
T2-3 (Seagrass)	<i>Ruppia maritima</i>	56	0.26	0.16	57
T2-5	none	22	-	-	22
T3-1 (Marsh)	<i>Juncus spp</i>	20	48	30	97
T3-3 (Seagrass)	<i>Ruppia maritima</i>	18	0.26	0.16	18
T3-5	none	13	-	-	13

4.5.3 Total Carbon Stock

The total carbon stock at each site can be assessed by summing the aboveground and belowground biomass and the sediment carbon (Figure 4.8 and Table 4.3). It should be noted that it is impossible to directly compare the carbon stocks found in this study to the global values because standard carbon stocks are calculated to a depth of 1m. The living biomass of all marsh cores is smaller than the sediment carbon stock, which is consistent with literature values. Seagrass values are also similar to values seen worldwide with living biomass representing only a fraction of the total carbon.

The total sediment carbon stock of one of the marsh cores (T2-1) has a value of 215MgC/ha, which greater than the sediments of the boreal, temperate, and tropical rainforests at 150-170MgC/ha (Fourqurean et al., 2012). Given that the core potentially only represents half of the carbon for 1m depth, it suggests that this marsh could sequester more than these ecosystems. The total carbon stocks of sites with seagrasses fall below the global average even after they are doubled. This indicates that seagrasses of Patos Lagoon sequester less carbon than is seen worldwide. All of the unvegetated sediment cores from this study are less than half of the literature value. It should be noted that the carbon stock value used for unvegetated sediment is taken from a singular study in the North Atlantic and is likely not the best representation of an averaged global value (Choi and Wang, 2004). Overall, the carbon stocks measured in Patos Lagoon appear to be less than global averages, but better sampling biomass sampling techniques and 1m-long sediment cores are needed to accurately assess the total carbon stock of these ecosystems.

The total ecosystem carbon stock was calculated to a depth of 50m using the known areas of marsh and seagrass beds in Patos Lagoon of 300km² and 120km², respectively (Table 4.4). The marshes store more carbon than seagrass beds given their greater area and higher average carbon density, with values ranging from 680,000 to 1,600,000MgC. Seagrass values are lower and range from 210,000 to 680,000 Mg of carbon. These values are preliminary estimates with major assumptions made about vegetation and sediment uniformity across the ecosystem area. This is asserted by the high % standard deviation values for all ecosystem carbon estimates, ranging from 25 to 78%. A higher sampling frequency and vegetation maps are needed to calculate better ecosystem carbon estimates.

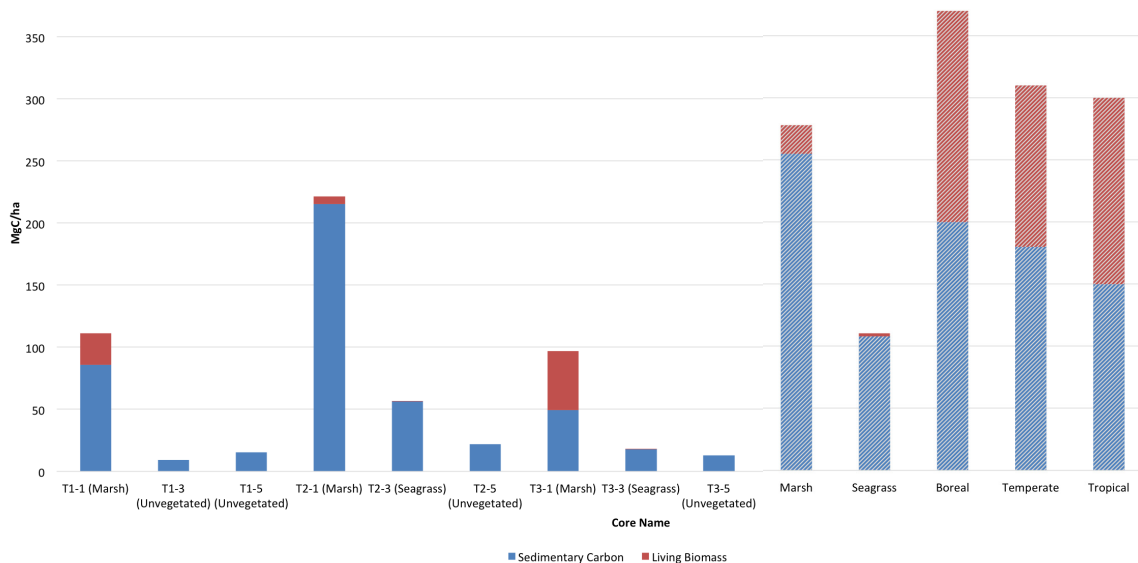


Figure 4.8: Total carbon stocks for each site are given by combining living biomass (aboveground) and sediment carbon (sediment and belowground) values (MgC/ha). Literature values for unvegetated (Choi and Wang, 2004), marsh (Elsley-Quirk et al., 2011; Howard et al., 2014), Seagrass (Howard et al., 2014), boreal forest, temperate forest, and tropical forest (Fourqurean et al., 2012).

Core	Species	Total Ecosystem Area (km ²)	Total Ecosystem Carbon (MgC)	Standard Deviation (MgC)	% Standard Deviation
T1-1	<i>Spartina densiflora</i>	300	770,000	200,000	25
T2-1	<i>Scirpus maritimus</i>	300	1,600,000	910,000	59
T2-3	<i>Ruppia maritima</i>	120	680,000	280,000	42
T3-1	<i>Juncus spp</i>	300	680,000	520,000	78
T3-3	<i>Ruppia maritima</i>	120	210,000	100,000	46

4.6 Significance

Carbon sequestered in marshes appears to largely reflect the in situ vegetation suggesting that the source of the carbon is the marsh itself. Seagrass beds are more difficult to interpret, but appear to reflect a combination of sources including the in situ vegetation, macroalgae, benthic microalgae, and phytoplankton. The carbon buried in unvegetated sediments is isotopically similar to the seagrass sediments indicating that the carbon is similarly sourced. All of these carbon sources appear to be largely estuarine based (the isotopic signature of the sediments reflect the sources outlined in Figure 4.1) implying that the carbon from these cores is sourced locally and not double counted from another ecosystem. This indicates that the coastal blue carbon in these coastal ecosystems makes them currently uncounted carbon stocks.

The sequestration ability of these ecosystems also make them good carbon sinks. While burial rates of seagrass beds measured in the study are below average, they are higher than other terrestrial ecosystems, which have been traditionally the largest carbon sinks and are included in carbon accounting schemes. Rough estimates of the carbon pools of these sediments are also somewhat comparable to these ecosystems in other parts of the world. These data argue that the salt marshes, seagrass beds, and unvegetated coastal sediments of Patos Lagoon are significant carbon stocks.

With development increasing around the Patos Lagoon Estuary system, these ecosystems face serious threats of degradation. A better understanding of the carbon stocks of these ecosystems has revealed that preserving them could provide not just ecological benefits, but economic benefits to the region. Brazil has long been at the forefront of the global carbon market with its leading role in the Clean Development Mechanism (CDM) policy. This policy, created during the Kyoto Protocol, allows for businesses or industries to earn carbon credits by reducing emissions. These credits are often acquired by developing nations and then sold to developed nations (largely in Europe) to help them meet stricter emissions standards (Hultman et al., 2012). This has created a thriving carbon market in Brazil with the Universidade Federal do Rio de Janeiro reporting that the country earned up to \$3 billion in 2012 from trading its carbon credits to other nations (Lozano, 2006). This mindset has already influenced thought about the preservation carbon sinks throughout Brazil such as encouraging afforestation and reforestation projects in the Amazon as well as broadening the scope of REDD+ projects (Hultman et al., 2012). It is also advantageous for Brazil to continue to protect their carbon sinks because being a net seller of credits

allows them to continue profiting off of selling them to other developed countries trying to reach quotas.

Currently Brazil is not marketing carbon from its blue carbon ecosystems. Based on the data from this study, it can be argued that the marshes, seagrasses, and marginal sediments in Patos Lagoon should be considered valuable carbon stocks. Given the large areas of marshes and seagrass beds in both Patos Lagoon and the rest of Brazil, it would be advantageous to promote conservation and further study of these ecosystems to better constrain the scope of these carbon sinks.

References

- Asmus, M., 1997, *Coastal plain and Patos Lagoon, Subtropical Convergence Environments*, Springer, p. 9-12.
- Baumgarten, M., Niencheski, L., and Veeck, L., 2001, Nutrientes na coluna da água e na água intersticial de sedimentos de uma enseada rasa estuarina com aportes de origem antrópica (RS-Brasil): *Atlântica*, v. 23, p. 101-116.
- Beck, M. W., Kenneth L. Heck, J. R., Able, K. W., Childers, D. L., Eggleston, D. B., Gillanders, B. M., Halpern, B., Hays, C. G., Hoshino, K., Minello, T. J., Orth, R. J., Sheridan, P. F., and Weinstein, M. P., 2001, *The Identification, Conservation, and Management of Estuarine and Marine Nurseries for Fish and Invertebrates: BioScience*, v. 51, no. 8, p. 633-641.
- Calliari, L., Garcia, C., Niencheski, L., Baumgarten, M., Costa, C., Seeliger, U., Abreu, P., Odebrecht, C., Montú, M., and Duarte, A., 1997, *Environment and biota of the Patos Lagoon Estuary, Subtropical Convergence Environments*, Springer, p. 13-64.
- Canadell, J. G., and Raupach, M. R., 2008, *Managing Forests for Climate Change Mitigation: Science*, v. 320, no. 5882, p. 1456-1457.
- Chanton, J. P., Martens, C. S., and Kipphut, G. W., 1983, Lead-210 sediment geochronology in a changing coastal environment: *Geochimica et Cosmochimica Acta*, v. 47, no. 10, p. 1791-1804.
- Chmura, G., and Aharon, P., 1995, Stable carbon isotope signatures of sedimentary carbon in coastal wetlands as indicators of salinity regime: *Journal of Coastal Research*, p. 124-135.
- Chmura, G. L., Anisfeld, S. C., Cahoon, D. R., and Lynch, J. C., 2003, Global carbon sequestration in tidal, saline wetland soils: *Global Biogeochemical Cycles*, v. 17, no. 4, p. 1111.
- Choi, Y., Wang, Y., Hsieh, Y. P., and Robinson, L., 2001, Vegetation succession and carbon sequestration in a coastal wetland in northwest Florida: Evidence from carbon isotopes: *Global Biogeochemical Cycles*, v. 15, no. 2, p. 311-319.
- Cole, M. L., Kroeger, K. D., McClelland, J. W., and Valiela, I., 2005, Macrophytes as indicators of land-derived wastewater: Application of a $\delta^{15}\text{N}$ method in aquatic systems: *Water Resources Research*, v. 41, no. 1.
- Cole, M. L., Valiela, I., Kroeger, K. D., Tomasky, G. L., Cebrian, J., Wigand, C., McKinney, R. A., Grady, S. P., and Carvalho da Silva, M. H., 2004, Assessment of a $\delta^{15}\text{N}$ Isotopic Method to Indicate Anthropogenic Eutrophication in Aquatic Ecosystems: *Journal of Environmental Quality*, v. 33, no. 1, p. 124-132.
- Costa, C., Seeliger, U., Oliveira, C., and Mazo, A., 1997, Distribuição, funções e valores das marismas e pradarias submersas no estuário da Lagoa dos Patos (RS, Brasil): *Atlântica*, v. 19, p. 65-83.
- Cundy, A. B., and Croudace, I. W., 1996, Sediment Accretion and Recent Sea-level Rise in the Solent, Southern England: Inferences from Radiometric and Geochemical Studies: *Estuarine, Coastal and Shelf Science*, v. 43, no. 4, p. 449-467.
- Cundy, A. B., Croudace, I. W., Thomson, J., and Lewis, J. T., 1997, Reliability of salt marshes as 'geochemical recorders' of pollution input: A case study from contrasting estuaries in southern England: *Environmental Science and Technology*, v. 31, no. 4, p. 1093-1101.
- Da Silva Copertino, M., 2011, Add coastal vegetation to the climate critical list: *Nature*, v. 473, no. 7347, p. 255-255.
- Davies, B., and Alloway, B., 1990, *Em Heavy Metals in Soils Lead: Heavy Metals in Soils Lead*.
- Elsey-Quirk, T., Seliskar, D. M., Sommerfield, C. K., and Gallagher, J. L., 2011, Salt Marsh Carbon Pool Distribution in a Mid-Atlantic Lagoon, USA: Sea Level Rise Implications: *Wetlands*, v. 31, no. 1, p. 87-99.
- Emerson, S., and Hedges, J. I., 1988, Processes controlling the organic carbon content of open ocean sediments: *Paleoceanography*, v. 3, no. 5, p. 621-634.
- Farber, S., Naeem, S., Raskin, R. G., Sutton, P., de Groot, R., Limburg, K., Paruelo, J., van den Belt, M., Hannon, B., d'Arge, R., Costanza, R., O'Neill, R. V., and Grasso, M., 1997, The value of the world's ecosystem services and natural capital: *Nature*, v. 387, no. 6630, p. 253-260.
- Fernandes, E. H. L., Dyer, K. R., Moller, O., and Niencheski, L. F. H., 2002, The Patos lagoon hydrodynamics during an El Nino event (1998): *Continental Shelf Research*, v. 22, no. 11, p. 1699-1713.
- Fogel, M. L., and Cifuentes, L. A., 1993, Isotope fractionation during primary production, *Organic geochemistry*, Springer, p. 73-98.
- Fourqurean, J. W., Duarte, C. M., Kennedy, H., Marbà, N., Holmer, M., Mateo, M. A., Apostolaki, E. T., Kendrick, G.

- A., Krause-Jensen, D., McGlathery, K. J., and Serrano, O., 2012, *Seagrass ecosystems as a globally significant carbon stock: Nature Geoscience*, v. 5, no. 7, p. 505-509.
- Fry, B., 1991, *Stable Isotope Diagrams of Freshwater Food Webs: Ecology*, v. 72, no. 6, p. 2293-2297.
- Fry, B., Scalan, R. S., and Parker, P. L., 1977, *Stable carbon isotope evidence for two sources of organic matter in coastal sediments: seagrasses and plankton: Geochimica et Cosmochimica Acta*, v. 41, no. 12, p. 1875-1877.
- Galimov, E., 2012, *The biological fractionation of isotopes*, Elsevier.
- Goericke, R., and Fry, B., 1994, *Variations of marine plankton $\delta^{13}C$ with latitude, temperature, and dissolved CO₂ in the world ocean: Global Biogeochemical Cycles*, v. 8, no. 1, p. 85-90.
- Goni, M. A., Ruttenberg, K. C., and Eglinton, T. I., 1997, *Sources and contribution of terrigenous organic carbon to surface sediments in the Gulf of Mexico: Nature [H.W. Wilson - GS]*, v. 389, p. 275.
- Grimm, A. M., Ferraz, S. E. T., and Gomes, J., 1998, *Precipitation anomalies in southern Brazil associated with El Nino and La Nina events: Journal of Climate*, v. 11, no. 11, p. 2863-2880.
- Harris, C. J., Beverly, William; Ambrose, William; Bourque, Bruce; Steneck, Robert; Dostie, Philip, 2016, *Stable Isotopic Shifts in Late Holocene Fish Bones from Archaeological Coastal Middens in Penobscot, Maine*.
- Hedges, J. I., 1992, *Global biogeochemical cycles: progress and problems: Marine Chemistry*, v. 39, no. 1-3, p. 67-93.
- Hedges, J. I., Clark, W. A., and Cowie, G. L., 1988, *Fluxes and Reactivities of Organic Matter in a Coastal Marine Bay: Limnology and Oceanography*, v. 33, no. 5, p. 1137-1152.
- Hendriks, I. E., Sintes, T., Bouma, T. J., and Duarte, C. M., 2008, *Experimental assessment and modeling evaluation of the effects of the seagrass Posidonia oceanica on flow and particle trapping: Marine Ecology Progress Series*, v. 356, p. 163-173.
- Hobbie, E. A., and Ouimette, A. P., 2009, *Controls of nitrogen isotope patterns in soil profiles: Biogeochemistry*, v. 95, no. 2-3, p. 355-371.
- Howard, J., Hoyt, S., Isensee, K., Telszewski, M., and Pidgeon, E., 2014, *Coastal blue carbon: methods for assessing carbon stocks and emissions factors in mangroves, tidal salt marshes, and seagrasses*.
- Hultman, N. E., Pulver, S., Guimaraes, L., Deshmukh, R., and Kane, J., 2012, *Carbon market risks and rewards: Firm perceptions of CDM investment decisions in Brazil and India: Energy Policy*, v. 40, no. 1, p. 90-102.
- Iacono, C. L., Mateo, M. A., Gràcia, E., Guasch, L., Carbonell, R., Serrano, L., Serrano, O., and Dañobeitia, J., 2008, *Very high-resolution seismo-acoustic imaging of seagrass meadows (Mediterranean Sea): Implications for carbon sink estimates: Geophysical Research Letters*, v. 35, no. 18, p. L18601.
- Johnson, B. J., Moore, K. A., Lehmann, C., Bohlen, C., and Brown, T. A., 2007, *Middle to late Holocene fluctuations of C3 and C4 vegetation in a Northern New England Salt Marsh, Sprague Marsh, Phippsburg Maine: Organic Geochemistry*, v. 38, no. 3, p. 394-403.
- Juracek, K. E., and Ziegler, A. C., 2006, *The legacy of leaded gasoline in bottom sediment of small rural reservoirs: Journal of environmental quality*, v. 35, no. 6, p. 2092-2102.
- Kennedy, H., Beggins, J., Duarte, C. M., Fourqurean, J. W., Holmer, M., Marbà, N., and Middelburg, J. J., 2010, *Seagrass sediments as a global carbon sink: Isotopic constraints: Global Biogeochemical Cycles*, v. 24, no. 4.
- Kjerfve, B., 1986, *Comparative oceanography of coastal lagoons: Estuarine variability*, v. 6381.
- Kreitler, C. W., and Browning, L. A., 1983, *Nitrogen-isotope analysis of groundwater nitrate in carbonate aquifers: Natural sources versus human pollution: Journal of Hydrology*, v. 61, no. 1-3, p. 285-301.
- Lee, S. V., and Cundy, A. B., 2001, *Heavy Metal Contamination and Mixing Processes in Sediments from the Humber Estuary, Eastern England: Estuarine, Coastal and Shelf Science*, v. 53, no. 5, p. 619-636.
- Leonard, L. A., and Luther, M. E., 1995, *Flow Hydrodynamics in Tidal Marsh Canopies: Limnology and Oceanography*, v. 40, no. 8, p. 1474-1484.
- Lovei, M., 1998, *Phasing out lead from gasoline: worldwide experience and policy implications*, World Bank Publications.
- Lozano, L., 2006, *Environmental finance: Brazil pioneers carbon credits market: London, Euromoney Institutional Investor PLC*, p. 1.
- Macko, S., 1994, *Pollution studies using stable isotopes: Stable isotopes in ecology and environmental science*, p. 45-62.
- McLeod, E., Chmura, G. L., Bouillon, S., Salm, R., Björk, M., Duarte, C. M., Lovelock, C. E., Schlesinger, W. H., and Silliman, B. R., 2011, *A blueprint for blue carbon: toward an improved understanding of the role of vegetated coastal habitats in sequestering CO₂: Frontiers in Ecology and the Environment*, v. 9, no. 10, p. 552-560.
- Medeiros, P. M., Bicego, M. C., Castelao, R. M., Del Rosso, C., Fillmann, G., and Zamboni, A. J., 2005, *Natural and*

- anthropogenic hydrocarbon inputs to sediments of Patos Lagoon Estuary, Brazil: Environment International*, v. 31, no. 1, p. 77-87.
- Meyers, P. A., 1994, *Preservation of elemental and isotopic source identification of sedimentary organic matter: Chemical Geology*, v. 114, no. 3, p. 289-302.
- Meyers, P. A., 1997, *Organic geochemical proxies of paleoceanographic, paleolimnologic, and paleoclimatic processes: Organic Geochemistry*, v. 27, no. 5, p. 213-250.
- Middelburg, J. J., Nieuwenhuize, J., Lubberts, R. K., and van de Plassche, O., 1997, *Organic Carbon Isotope Systematics of Coastal Marshes: Estuarine, Coastal and Shelf Science*, v. 45, no. 5, p. 681-687.
- Möller, O. O., Castaing, P., Salomon, J.-C., and Lazure, P., 2001, *The Influence of Local and Non-Local Forcing Effects on the Subtidal Circulation of Patos Lagoon: Estuaries*, v. 24, no. 2, p. 297-311.
- Moller, O. O., Lorenzenti, J. o. A., Stech, J., and Math, M. M., 1996, *The Patos Lagoon summertime circulation and dynamics: Continental Shelf Research*, v. 16, no. 3, p. 335-351.
- Müller, P. J., and Suess, E., 1979, *Productivity, sedimentation rate, and sedimentary organic matter in the oceans-I. Organic carbon preservation: Deep Sea Research Part A, Oceanographic Research Papers*, v. 26, no. 12, p. 1347-1362.
- Niencheski, L. F., Moore, W. S., and Windom, H. L., 2014, *History of human activity in coastal southern Brazil from sediment: Marine Pollution Bulletin*, v. 78, no. 1-2, p. 209-212.
- Nixon, S. W., 1982, *The ecology of New England high salt marshes: a community profile (Spartina)*, v. Book, Whole.
- O'Leary, M. H., 1988, *Carbon Isotopes in Photosynthesis: BioScience*, v. 38, no. 5, p. 328-336.
- Odebrecht, C., Abreu, P., Bemvenuti, C., Copertino, M., Muelbert, J., Vieira, J., and Seeliger, U., 2010, *The Patos Lagoon Estuary: biotic responses to natural and anthropogenic impacts in the last decades (1979–2008): Coastal Lagoons: Critical Habitats of Environmental Change*, p. 437-459.
- Orth, R. J., Tim J. B. C., Dennison, W. C., Duarte, C. M., Fourqurean, J. W., Kenneth L. Heck, J. R., Hughes, A. R., Kendrick, G. A., Kenworthy, W. J., Olyarnik, S., Short, F. T., Waycott, M., and Williams, S. L., 2006, *A Global Crisis for Seagrass Ecosystems: BioScience*, v. 56, no. 12, p. 987-996.
- Papadimitriou, S., Kennedy, D. P., Kennedy, H., Duarte, C. M., and Marbà, N., 2005, *Sources of organic matter in seagrass-colonized sediments: A stable isotope study of the silt and clay fraction from Posidonia oceanica meadows in the western Mediterranean: Organic Geochemistry*, v. 36, no. 6, p. 949-961.
- Pendleton, L., Donato, D. C., Murray, B. C., Crooks, S., Jenkins, W. A., Sifleet, S., Craft, C., Fourqurean, J. W., Kauffman, J. B., Marbà, N., Magonigal, P., Pidgeon, E., Herr, D., Gordon, D., and Baldera, A., 2012, *Estimating Global “Blue Carbon” Emissions from Conversion and Degradation of Vegetated Coastal Ecosystems: PLoS ONE* v. 7, no. 9, p. e43542.
- Peterson, B. J., and Fry, B., 1987, *Stable Isotopes in Ecosystem Studies: Annual Review of Ecology and Systematics*, v. 18, no. 1, p. 293-320.
- Peterson, B. J., Howarth, R. W., and Garritt, R. H., 1985, *Multiple Stable Isotopes Used to Trace the Flow of Organic Matter in Estuarine Food Webs: Science*, v. 227, no. 4692, p. 1361-1363.
- , 1986, *Sulfur and Carbon Isotopes as Tracers of Salt-Marsh Organic Matter Flow: Ecology*, v. 67, no. 4, p. 865-874.
- Prahl, F. G., and Muehlhausen, L. A., 1989, *Lipid biomarkers as geochemical tools for paleoceanographic study.*
- Sarkar, S., Ahmed, T., Swami, K., Judd, C. D., Bari, A., Dutkiewicz, V. A., and Husain, L., 2015, *History of atmospheric deposition of trace elements in lake sediments, ~1880 to 2007: Journal of Geophysical Research: Atmospheres*, v. 120, no. 11, p. 5658-5669.
- Schoeninger, M. J., and DeNiro, M. J., 1984, *Nitrogen and carbon isotopic composition of bone collagen from marine and terrestrial animals: Geochimica et Cosmochimica Acta*, v. 48, no. 4, p. 625-639.
- Seeliger, U., and Kjerfve, B., 2000, *Coastal marine ecosystems of Latin America, Springer Science & Business Media.*
- Sharp, Z., 2007, *Principles of stable isotope geochemistry*, Pearson Education Upper Saddle River, NJ.
- Tagliani, P., Landazuri, H., Reis, E., Tagliani, C., Asmus, M., and Sanchez-Arcilla, A., 2003, *Integrated coastal zone management in the Patos Lagoon estuary: perspectives in context of developing country: Ocean & Coastal Management*, v. 46, no. 9, p. 807-822.
- Tagliani, P. R., and Asmus, M. L., 1997, *Estudo de impacto ambiental do Porto de Rio Grande, RS: Relatório Final*, v. 1.
- Tiessen, H., Karamanos, R., Stewart, J., and Selles, F., 1984, *Natural nitrogen-15 abundance as an indicator of soil organic matter transformations in native and cultivated soils: Soil Science Society of America Journal*, v. 48,

- no. 2, p. 312-315.
- Toldo, E. E., Jr., Dillenburg, S. R., Correa, I. C. S., and Almeida, L., 2000, *Holocene Sedimentation in Lagoa dos Patos Lagoon, Rio Grande do Sul, Brazil: Journal of Coastal Research*, v. 16, no. 3, p. 816-822.
- Trennepohl, N., 2010, *Brazil's Policy on Climate Change: Recent Legislation and Challenges to Implementation: Carbon & Climate Law Review : CCLR*, v. 4, no. 3, p. 271.
- Tyson, R. V., 1995, *Bulk Geochemical Characterization and Classification of Organic Matter: Stable Carbon Isotopes ($\delta^{13}C$), Sedimentary Organic Matter*, Springer, p. 395-416.
- United Nations Environment, P., 2010, *UNEP 2009 Annual Report: Seizing the Green Opportunity; 2010 IIS 4230-S3; DCP/1250/NA; ISSN 1010-1268; ISBN 978-92-807-3071-5*.
- USEPA, 2000, *National air pollutant emission trends, 1900-1998*.
- Villwock, J. A., 1984, *Geology of the coastal province of Rio Grande do Sul, Southern Brazil: A synthesis. Pesquisas*, v. 16, p. 5-49.
- Vizzini, S., Sarà, G., Michener, R. H., and Mazzola, A., 2002, *The role and contribution of the seagrass *Posidonia oceanica* (L.) Delile organic matter for secondary consumers as revealed by carbon and nitrogen stable isotope analysis: Acta Oecologica*, v. 23, no. 4, p. 277-285.
- Weinstein, M. P., Litvin, S. Y., Bosley, K. L., Fuller, C. M., and Wainright, S. C., 2000, *The role of tidal salt marsh as an energy source for marine transient and resident finfishes: a stable isotope approach: Transactions of the American Fisheries Society*, v. 129, no. 3, p. 797-810.

Appendices

Appendix 1

<i>Spartina densiflora</i> Geochemical Data										
Species Name	Sample Type	Dry Mass (g)	Sample Area (cm ²)	% N	N (umoles)	d15N (permil)	%C	C (umoles)	d13C (permil)	C/N (Molar)
<i>Spartina densiflora</i>	Aboveground	46.31	78.5	0.63	1.93	5.74	43.02	152.97	-13.39	79.15
<i>Spartina densiflora</i>	Belowground	195.03	78.5	0.44	1.70	4.65	17.86	79.79	-15.44	46.89

<i>Scirpus maritimus</i> Geochemical Data										
Species Name	Sample Type	Dry Mass (g)	Sample Area (cm ²)	% N	N (umoles)	d15N (permil)	%C	C (umoles)	d13C (permil)	C/N (Molar)
<i>Scirpus maritimus</i>	Aboveground	10.59	78.5	1.08	3.18	5.12	45.47	155.62	-26.06	48.87
<i>Scirpus maritimus</i>	Aboveground	7.26	78.5	0.42	1.01	4.09	43.13	120.88	-25.36	119.17
<i>Scirpus maritimus</i>	Aboveground	16.75	78.5	0.42	1.01	4.09	43.13	120.88	-25.36	119.17
<i>Scirpus maritimus</i>	Belowground	24.21	78.5	1.05	2.71	4.39	41.10	123.25	-25.98	45.41
<i>Scirpus maritimus</i>	Belowground	138.87	78.5	0.88	3.32	3.98	38.30	166.38	-25.04	50.11
<i>Scirpus maritimus</i>	Belowground	235.01	78.5	1.22	3.52	4.36	40.06	133.40	-25.25	37.95

<i>Juncus</i> spp Geochemical Data										
Species Name	Sample Type	Dry Mass (g)	Sample Area (cm ²)	% N	N (umoles)	d15N (permil)	%C	C (umoles)	d13C (permil)	C/N (Molar)
<i>Juncus</i> spp	Aboveground	105.73	78.5	1.12	1.53	5.02	43.20	68.54	-29.86	44.93
<i>Juncus</i> spp	Aboveground	31.06	78.5	1.36	3.26	4.23	44.75	124.79	-30.89	38.22
<i>Juncus</i> spp	Aboveground	113.09	78.5	1.34	2.14	3.43	46.41	85.69	-29.55	40.09
<i>Juncus</i> spp	Belowground	44.68	78.5	1.05	2.80	4.33	41.04	126.81	-28.60	45.27
<i>Juncus</i> spp	Belowground	18.43	78.5	0.84	1.53	4.17	36.72	77.15	-29.19	50.44
<i>Juncus</i> spp	Belowground	119.14	78.5	0.87	2.83	4.27	37.95	142.26	-28.06	50.32

<i>Ruppia maritima</i> Geochemical Data												
Species Name	Sample Type	Dry Mass (g)	Sample Area (cm ²)	% N	N (umoles)	d15N (permil)	%C	C (umoles)	d13C (permil)	C/N (Molar)		
<i>Ruppia maritima</i>	Aboveground	0.73	78.5	2.88	6.13	3.91	40.22	81.58	-13.91	13.30		
<i>Ruppia maritima</i>	Aboveground	0.67	78.5	2.46	6.44	4.32	31.66	83.97	-17.60	13.05		
<i>Ruppia maritima</i>	Aboveground	1.26	78.5	2.96	6.40	4.54	35.00	82.72	-17.28	12.92		
<i>Ruppia maritima</i>	Aboveground	0.80	78.5	2.87	8.43	4.26	25.88	105.99	-14.84	12.57		
<i>Ruppia maritima</i>	Aboveground	0.43	78.5	3.07	9.86	4.57	38.80	122.94	-16.13	12.47		
<i>Ruppia maritima</i>	Aboveground	0.45	78.5	2.26	6.32	3.62	32.02	96.39	-15.46	15.26		
<i>Ruppia maritima</i>	Aboveground	0.22	78.5	2.71	4.82	3.17	39.45	67.70	-14.23	14.06		
<i>Ruppia maritima</i>	Aboveground	0.25	78.5	2.86	6.93	3.63	27.10	96.72	-15.22	13.95		
<i>Ruppia maritima</i>	Aboveground	0.13	78.5	2.75	5.85	4.54	33.24	77.77	-17.19	13.30		
<i>Ruppia maritima</i>	Belowground	0.43	78.5	1.52	2.94	3.35	37.64	57.95	-14.56	19.73		
<i>Ruppia maritima</i>	Belowground	0.51	78.5	1.50	2.55	3.82	38.58	41.86	-17.28	16.45		
<i>Ruppia maritima</i>	Belowground	0.36	78.5	1.71	3.45	3.50	26.27	62.92	-16.91	18.22		
<i>Ruppia maritima</i>	Belowground	0.49	78.5	1.30	5.42	3.44	40.28	103.54	-14.46	19.11		

<i>Ruppia maritima</i> Geochemical Data Continued											
Species Name	Sample Type	Dry Mass (g)	Sample Area (cm ²)	% N	N (umoles)	d15N (permil)	%C	C (umoles)	d13C (permil)	C/N (Molar)	
<i>Ruppia maritima</i>	Belowground	0.30	78.5	1.40	3.79	3.92	30.70	70.87	-15.34	18.70	
<i>Ruppia maritima</i>	Belowground	0.49	78.5	1.10	2.49	2.89	37.11	79.80	-15.39	32.08	
<i>Ruppia maritima</i>	Belowground	0.30	78.5	1.52	3.13	1.92	36.02	58.74	-14.89	18.77	
<i>Ruppia maritima</i>	Belowground	0.11	78.5	1.36	4.42	3.35	38.51	95.92	-14.61	21.70	
<i>Ruppia maritima</i>	Belowground	0.36	78.5	1.76	4.24	4.05	23.26	80.38	-17.02	18.97	

Appendix 2

Sediment Geochemical Data of Core T1-1										
Core Name	Depth Interval (cm)	Bulk Density (g/cm ³)	% N	N (umoles)	d15N (permil)	%C	C (umoles)	d13C (permil)	C/N	
T1-1	0-2	0.35	0.34	5.61	4.04	4.79	90.79	-16.48	16.17	
T1-1	2-4	0.31	0.35	6.01	3.82	5.39	107.84	-16.19	17.96	
T1-1	4-6	0.33	0.34	7.08	4.02	4.87	116.08	-16.36	16.40	
T1-1	6-8	0.32	0.35	10.00	4.24	4.47	146.10	-16.47	14.61	
T1-1	8-10	0.32	0.35	8.18	3.81	4.66	125.71	-16.40	15.36	
T1-1	10-12	0.31	0.35	9.78	3.62	4.87	157.10	-16.44	16.06	
T1-1	12-14	0.30	0.27	9.76	3.65	3.67	152.21	-16.62	15.59	
T1-1	14-16	0.55	0.14	5.31	3.48	1.98	88.81	-17.20	16.71	
T1-1	16-18	0.54	0.10	5.27	3.70	1.47	85.61	-17.22	16.24	
T1-1	18-20	0.64	0.09	4.59	3.82	1.25	74.06	-17.37	16.14	
T1-1	20-25	0.65	0.07	3.97	4.34	0.85	54.68	-17.37	13.79	
T1-1	25-30	0.67	0.05	3.15	4.90	0.57	40.63	-17.68	12.91	
T1-1	30-35	0.74	0.04	2.79	5.23	0.42	32.13	-17.36	11.52	
T1-1	35-40	0.79	0.03	1.87	5.63	0.36	23.70	-17.65	12.69	
T1-1	40-45	0.80	0.03	2.00	5.10	0.32	24.46	-18.21	12.21	
T1-1	45-50	0.69	0.04	2.32	5.38	0.35	26.95	-18.23	11.60	

Sediment Geochemical Data of Core T1-3										
Core Name	Depth Interval (cm)	Bulk Density (g/cm ³)	% N	N (umoles)	d15N (permil)	%C	C (umoles)	d13C (permil)	C/N	
T1-3	0-2	1.24	0.03	1.24	7.36	0.19	9.06	-16.99	7.29	
T1-3	2-4	0.98	0.02	0.76	7.18	0.15	5.77	-17.62	7.59	
T1-3	4-6	0.82	0.02	1.04	7.54	0.16	8.45	-18.14	8.12	
T1-3	6-8	0.79	0.02	1.01	7.81	0.15	7.98	-17.89	7.91	
T1-3	8-10	0.72	0.02	0.66	6.93	0.13	5.42	-18.38	8.18	
T1-3	10-12	0.86	0.02	0.64	6.82	0.12	5.22	-18.43	8.13	
T1-3	12-14	0.84	0.01	0.67	7.27	0.11	5.92	-18.60	8.83	
T1-3	14-16	0.93	0.02	0.64	5.99	0.13	6.25	-17.96	9.76	
T1-3	16-18	0.69	0.03	1.06	6.27	0.22	10.61	-17.05	10.05	
T1-3	18-20	0.83	0.03	1.43	6.60	0.25	14.46	-17.44	10.11	
T1-3	20-25	0.70	0.03	1.70	6.60	0.29	17.14	-17.35	10.09	
T1-3	25-30	0.78	0.04	1.91	6.54	0.45	27.92	-14.06	14.58	
T1-3	30-35	0.68	0.03	1.65	6.49	0.31	19.63	-15.70	11.91	
T1-3	35-40	0.70	0.03	1.61	6.91	0.28	20.11	-14.66	12.52	
T1-3	40-45	0.77	0.03	1.69	6.98	0.30	20.37	-14.82	12.05	
T1-3	45-50	0.88	0.02	1.31	7.32	0.25	16.82	-13.59	12.81	

Sediment Geochemical Data of Core T1-5										
Core Name	Depth Interval (cm)	Bulk Density (g/cm ³)	% N	N (umoles)	d15N (permil)	%C	C (umoles)	d13C (permil)	C/N	
T1-5	0-2	0.78	0.06	2.39	7.20	0.41	20.36	-18.68	8.50	
T1-5	2-4	0.79	0.04	1.44	7.33	0.29	11.93	-18.98	8.27	
T1-5	4-6	0.77	0.04	1.63	7.21	0.30	13.82	-18.92	8.47	
T1-5	6-8	0.80	0.03	1.02	6.83	0.21	8.62	-19.14	8.42	
T1-5	8-10	0.81	0.02	0.88	6.74	0.20	8.17	-19.54	9.32	
T1-5	10-12	0.95	0.03	1.03	6.40	0.22	10.23	-18.15	9.95	
T1-5	12-14	0.87	0.04	1.40	6.29	0.38	14.97	-16.93	10.67	
T1-5	14-16	0.66	0.05	1.76	6.09	0.42	17.96	-17.33	10.20	
T1-5	16-18	0.65	0.07	2.58	5.90	0.67	30.00	-15.97	11.65	
T1-5	18-20	0.59	0.06	3.24	6.30	0.58	33.87	-17.44	10.46	
T1-5	20-25 (a)	0.64	0.07	3.83	6.14	0.65	40.29	-17.02	10.52	
T1-5	25-30	0.57	0.06	3.71	6.52	0.53	38.39	-16.95	10.36	
T1-5	30-35	0.56	0.06	3.43	6.73	0.69	42.90	-15.65	12.50	
T1-5	35-40	0.68	0.05	2.65	7.07	0.49	30.79	-14.57	11.60	
T1-5	40-45	0.67	0.04	2.54	7.70	0.44	35.14	-11.91	13.82	

Sediment Geochemical Data of Core T2-1										
Core Name	Depth Interval (cm)	Bulk Density (g/cm ³)	% N	N (umoles)	d15N (permil)	%C	C (umoles)	d13C (permil)	C/N	
T2-1	0-2	1.22	0.65	10.70	3.29	9.05	173.62	-25.83	16.22	
T2-1	2-4	0.47	0.60	10.62	3.71	8.79	179.23	-25.80	16.87	
T2-1	4-6	0.48	0.58	12.22	3.99	8.14	197.30	-25.71	16.15	
T2-1	6-8	0.47	0.60	11.13	3.75	8.91	191.83	-25.87	17.24	
T2-1	8-10	0.58	0.50	10.35	3.78	6.86	165.78	-25.59	16.02	
T2-1	10-12	0.49	0.46	12.47	3.91	6.29	196.39	-25.57	15.74	
T2-1	12-14	0.62	0.39	13.86	3.96	4.86	201.44	-25.07	14.54	
T2-1	14-16	0.78	0.34	13.66	4.25	4.30	198.08	-24.91	14.50	
T2-1	16-18	0.69	0.33	16.52	4.02	4.17	244.38	-24.94	14.79	
T2-1	18-20	0.74	0.32	15.03	4.20	3.94	215.97	-25.07	14.37	
T2-1	20-25	0.82	0.29	17.29	4.13	3.67	253.18	-25.51	14.64	
T2-1	25-30	1.01	0.21	10.86	4.50	3.22	196.14	-25.23	18.06	
T2-1	30-35	0.99	0.18	11.66	5.12	2.31	172.09	-24.24	14.76	
T2-1	35-40	1.32	0.13	9.52	4.90	1.97	167.49	-24.77	17.59	
T2-1	40-45	1.44	0.10	7.83	3.16	2.04	192.18	-25.60	24.53	
T2-1	45-50	1.54	0.07	5.97	3.57	1.55	152.09	-23.74	25.48	

Sediment Geochemical Data of Core T2-3										
Core Name	Depth Interval (cm)	Bulk Density (g/cm ³)	% N	N (umoles)	d15N (permil)	%C	C (umoles)	d13C (permil)	C/N	
T2-3	0-2	2.85	0.02	0.87	3.70	0.16	7.40	-18.58	8.52	
T2-3	2-4	1.88	0.02	0.74	3.57	0.15	7.54	-19.37	10.17	
T2-3	4-6	1.77	0.02	1.00	3.84	0.22	11.98	-19.62	12.01	
T2-3	6-8	1.54	0.06	2.34	4.08	0.64	31.65	-16.98	13.55	
T2-3	8-10	1.11	0.09	3.98	4.73	1.06	55.75	-16.37	13.99	
T2-3	10-12	1.23	0.10	3.76	4.99	1.26	52.76	-16.27	14.03	
T2-3	12-14	1.12	0.11	4.38	5.05	1.40	62.82	-15.78	14.35	
T2-3	14-16	1.20	0.10	4.59	4.86	1.32	68.84	-17.22	14.99	
T2-3	16-18	1.11	0.09	3.87	5.09	1.26	61.12	-16.05	15.80	
T2-3	18-20	1.26	0.10	4.51	5.10	1.40	73.80	-15.26	16.35	
T2-3	20-25	1.06	0.11	4.56	5.16	1.50	72.21	-15.85	15.82	
T2-3	25-30	1.22	0.09	5.83	5.66	1.22	86.69	-15.72	14.88	
T2-3	30-35	1.25	0.08	4.29	6.11	0.95	58.84	-17.17	13.72	
T2-3	35-40	1.22	0.08	4.19	6.37	0.80	51.02	-16.90	12.16	
T2-3	40-45	1.06	0.08	5.26	6.59	0.82	60.05	-17.85	11.41	
T2-3	45-50	1.16	0.07	3.67	6.76	0.63	40.83	-18.45	11.12	

Sediment Geochemical Data of Core T2-5										
Core Name	Depth Interval (cm)	Bulk Density (g/cm ³)	% N	N (umoles)	d15N (permil)	%C	C (umoles)	d13C (permil)	C/N	
T2-5	0-2	1.99	0.02	1.13	4.85	0.14	10.71	-18.52	9.45	
T2-5	2-4	1.87	0.02	1.01	4.86	0.13	9.44	-18.58	9.39	
T2-5	4-6	1.73	0.02	1.37	4.95	0.18	14.08	-17.78	10.24	
T2-5	6-8	1.76	0.02	1.16	4.55	0.17	12.43	-17.09	10.72	
T2-5	8-10	1.87	0.03	2.09	4.82	0.28	24.03	-16.84	11.49	
T2-5	10-12	1.49	0.03	1.99	4.84	0.29	22.05	-16.76	11.06	
T2-5	12-14	1.57	0.03	1.91	4.70	0.34	22.69	-16.98	11.91	
T2-5	14-16	1.46	0.04	3.00	4.85	0.46	37.02	-16.80	12.33	
T2-5	16-18	1.50	0.04	2.06	5.10	0.40	26.16	-16.81	12.73	
T2-5	18-20	1.65	0.03	2.03	5.16	0.46	32.38	-15.92	15.95	
T2-5	20-25	1.53	0.02	1.61	5.67	0.24	19.49	-18.37	12.13	
T2-5	25-30	1.67	0.02	1.44	5.49	0.16	15.33	-17.76	10.61	
T2-5	30-35	1.56	0.02	1.54	6.21	0.21	16.49	-17.93	10.67	
T2-5	35-40	1.44	0.04	2.60	6.62	0.34	28.40	-18.17	10.94	
T2-5	40-45	1.36	0.04	2.38	6.72	0.35	26.93	-17.88	11.31	
T2-5	45-50	1.08	0.05	3.30	6.78	0.52	41.39	-18.07	12.55	

Sediment Geochemical Data of Core T3-1										
Core Name	Depth Interval (cm)	Bulk Density (g/cm ³)	% N	N (umoles)	d15N (permil)	%C	C (umoles)	d13C (permil)	C/N	
T3-1	0-2	1.53	0.05	2.90	4.40	0.49	35.47	-23.24	12.24	
T3-1	2-4	1.13	0.02	1.36	3.85	0.19	16.46	-23.22	12.09	
T3-1	4-6	1.33	0.02	1.17	4.13	0.20	16.78	-24.53	14.34	
T3-1	6-8	1.24	0.03	2.24	4.24	0.41	39.77	-24.51	17.77	
T3-1	8-10	1.21	0.03	2.80	4.06	0.53	50.72	-25.45	18.12	
T3-1	10-12	1.25	0.03	1.71	4.00	0.40	30.41	-25.49	17.75	
T3-1	12-14	1.04	0.03	1.89	4.03	0.35	30.03	-26.15	15.91	
T3-1	14-16	1.22	0.02	1.61	4.35	0.29	26.04	-25.59	16.19	
T3-1	16-18	1.24	0.02	1.25	4.61	0.25	18.81	-25.06	15.04	
T3-1	18-20	1.35	0.01	0.94	4.98	0.16	12.22	-25.11	13.05	
T3-1	20-25	1.19	0.04	2.97	4.14	0.61	53.31	-25.77	17.98	
T3-1	25-30	1.25	0.03	2.38	4.80	0.55	47.27	-26.52	19.87	
T3-1	30-35	1.20	0.02	1.23	4.59	0.21	17.08	-23.15	13.83	
T3-1	35-40	1.48	0.01	0.96	3.87	0.13	10.52	-21.54	10.98	
T3-1	40-45	1.25	0.02	1.30	3.71	0.16	12.63	-20.82	9.73	
T3-1	45-49	1.14	0.01	1.02	3.92	0.12	10.19	-21.27	10.03	

Sediment Geochemical Data of Core T3-3										
Core Name	Depth Interval (cm)	Bulk Density (g/cm ³)	% N	N (umoles)	d15N (permil)	%C	C (umoles)	d13C (permil)	C/N	
T3-3	0-2	1.55	0.07	5.19	2.42	0.47	41.60	-18.40	8.01	
T3-3	2-4	1.72	0.03	2.27	2.79	0.22	18.23	-18.87	8.05	
T3-3	4-6	1.90	0.02	1.70	2.91	0.16	12.98	-18.80	7.65	
T3-3	6-8	2.06	0.02	1.59	3.13	0.14	12.76	-18.85	8.04	
T3-3	8-10	1.79	0.02	1.56	2.76	0.16	13.79	-18.39	8.86	
T3-3	10-12	1.95	0.02	1.24	2.95	0.11	10.02	-19.26	8.08	
T3-3	12-14	1.90	0.01	1.02	3.22	0.10	8.67	-19.38	8.52	
T3-3	14-16	1.90	0.01	0.91	3.17	0.08	7.85	-19.30	8.60	
T3-3	16-18	1.97	0.01	0.77	3.36	0.09	8.22	-21.25	10.66	
T3-3	18-20	1.86	0.01	0.82	3.16	0.11	9.34	-17.60	11.40	
T3-3	20-25	1.97	0.01	1.09	3.40	0.13	11.42	-17.15	10.49	
T3-3	25-30	1.74	0.03	1.84	4.34	0.24	19.82	-16.83	10.76	
T3-3	30-35	1.55	0.04	2.68	4.36	0.41	35.69	-16.78	13.32	
T3-3	35-40	1.74	0.02	1.58	4.30	0.20	16.87	-16.69	10.65	
T3-3	40-44	1.92	0.02	1.59	4.12	0.22	18.05	-17.30	11.32	

Sediment Geochemical Data of Core T3-5										
Core Name	Depth Interval (cm)	Bulk Density (g/cm ³)	% N	N (umoles)	d15N (permil)	%C	C (umoles)	d13C (permil)	C/N	
T3-5	0-2	1.43	0.02	1.25	3.65	0.15	12.30	-18.30	9.88	
T3-5	2-4	1.41	0.02	1.50	4.24	0.18	15.09	-17.04	10.09	
T3-5	4-6	1.20	0.03	2.17	4.81	0.22	19.03	-15.95	8.76	
T3-5	6-8	0.99	0.05	3.27	4.50	0.52	42.69	-16.46	13.06	
T3-5	8-10	0.80	0.06	5.13	4.44	0.59	57.00	-16.52	11.12	
T3-5	10-12	0.64	0.07	4.77	4.61	0.71	57.38	-16.98	12.02	
T3-5	12-14	0.51	0.08	6.07	4.43	0.84	72.32	-16.12	11.91	
T3-5	14-16	0.51	0.08	5.58	4.43	0.75	64.08	-16.45	11.48	
T3-5	16-18	0.46	0.06	4.17	3.79	0.58	48.68	-17.04	11.66	
T3-5	18-20	0.45	0.06	4.47	3.97	0.62	52.62	-16.60	11.77	
T3-5	20-25	0.39	0.05	4.44	4.88	0.49	49.33	-16.81	11.12	
T3-5	25-30	0.32	0.06	4.81	5.17	0.62	57.28	-16.96	11.91	
T3-5	30-35	0.26	0.07	4.71	5.29	0.69	57.52	-16.79	12.21	
T3-5	35-40	0.25	0.06	4.91	5.11	0.75	68.22	-15.07	13.90	
T3-5	40-45	0.24	0.05	3.95	5.03	0.58	51.19	-16.18	12.97	
T3-5	45-50	0.24	0.03	2.72	6.55	0.45	43.11	-13.66	15.83	

Appendix 3

Sediment Lead Concentration of T1-3					
Core Name	Depth Interval (cm)	Pb 220 (ppm)			
T1-3	0-1	2.19	T1-3	29-30	2.47
T1-3	1-2	2.56	T1-3	30-31	3.28
T1-3	2-3	4.86	T1-3	31-32	2.91
T1-3	3-4	2.61	T1-3	32-33	2.38
T1-3	4-5	2.65	T1-3	33-34	2.50
T1-3	5-6	2.25	T1-3	34-35	2.65
T1-3	6-7	2.34	T1-3	35-36	2.79
T1-3	7-8	2.11	T1-3	37-38	2.26
T1-3	8-9	2.53	T1-3	39-40	2.21
T1-3	9-10	3.37	T1-3	41-42	1.92
T1-3	10-11	3.34	T1-3	43-44	2.37
T1-3	11-12	3.38	T1-3	45-46	2.25
T1-3	12-13	3.83	T1-3	47-48	2.14
T1-3	13-14	3.64	T1-3	49-50	2.08
T1-3	14-15	4.39	T1-3	13-14	3.64
T1-3	15-16	3.79			
T1-3	16-17	4.21			
T1-3	17-18	3.57			
T1-3	18-19	3.76			
T1-3	19-20	4.20			
T1-3	20-21	3.69			
T1-3	21-22	3.11			
T1-3	22-23	3.08			
T1-3	23-24	2.75			
T1-3	24-25	3.04			
T1-3	25-26	3.49			
T1-3	26-27	3.48			
T1-3	27-28	2.82			
T1-3	28-29	2.76			

